ConsenCUS

Thermo-mechanical behaviour of rock salt in the context of gas storage: a review

ConsenCUS-D4.1-Review on the mechanical behaviour of rock salt in gas storage conditions – version 1 - 2112

Date	Version	Status	Initials	Changes Marked
16/12/2021	1	Final draft	AOS	
01/02/2022	2	Reviewed	NA	

This project has received funding from the European Union's Horizon 2020 research and Innovation programme under grant agreement N° 101022484.

Version Control Sheet

WP: WP3 CO2 Storage

Lead author: Nathaniel Forbes Inskip

Contributing Authors: Audrey Ougier-Simonin

Due date: 2021-10-31

Date: 2021-12-15

Version: 1

Contact: audreyo@bgs.ac.uk

Dissemination Level: ■ PU: Public

☐ CO: Confidential, only for members of the consortium (including the Commission)

Acknowledgments

The authors would like to thank Dr Carla Martin Clave, former PhD student in the Rock Mechanics and Physics Laboratory at the British Geological Survey, for her literature review work during her thesis. Her initial work has been immensely helpful to feed and shape this report.

The authors acknowledge the ConsenCUS project and all the partners involved for supporting this work. A special thanks to Dirk Koppert (NEC) and Nikolai Andrianov (GEUS) for reviewing this report.

The sole responsibility for the content of this publication lies with the authors. It does not necessarily represent the opinion of the European Union. Neither CINEA nor the European Commission are responsible for any use that may be made of the information contained therein.

Abstract

Salt caverns form an ideal reservoir for gas storage, and as such are extensively used for seasonal natural gas storage. Rock salt is indeed an ideal medium for such operations as it leaches easily, and so cavern construction is relatively simple, but it is also ductile, which reduces the risk of integrity and stability issues. Although reduced, the risks still exist, where brittle deformation from either thermal stresses or fatigue can lead to fracturing in the cavern walls, or ductile deformation (creep) can lead to cavern closure. The operational considerations for gas storage are quite different depending on the storage purpose: for seasonal gas storage, a cavern is usually only emptied and filled once a year, whereas for energy storage, or the temporary storage of CO_2, caverns may be emptied and filled on an hourly to daily basis. It may be possible to manage the associated risks by modifying the operating pressures within the cavern and gas fluxes in and out of the cavern. In order to properly assess these risks, the fundamental mechanisms of rock salt deformation, and their impact on permeability and cavern stability, need to be understood at the relevant pressure and temperature conditions for each scenario.

This study collates and reviews a large body of literature covering the different temporal and spatial scales that are important for the use of salt caverns for UGS, from rock salt formation and grain scale mechanics, to the reservoir scale and operational considerations. At the reservoir scale, the focus is on a more frequent cycling of gas, which is more relevant to energy storage (hydrogen and compressed air) and temporary storage of CO_2. Finally, we highlight where some knowledge gaps in the fundamental mechanisms of salt deformation still exist, and offer some suggestions on how to address these using laboratory experiments.

Table of contents

1 Introduction

Abating climate change requires a transition to a low carbon economy (IPCC 2014). Meeting the targets as set out in the Paris agreement and UN Sustainable Developments Goals 7, 9 and 13, will require both the energy, and heavy industries, to change at pace, which is a challenge and will be for years to come. While there has been a focus on decarbonising energy production for some time, to date, there has been comparatively little progress in the de-carbonisation of energy-intensive and large CO_2 emitting, heavy industries (such as oil and gas, steel, cement and waste processing). These industries are of vital, strategic importance to economies globally, and as such implementing low carbon solutions, such as Carbon Capture Utilisation and Storage (CCUS), within these industries, is of global importance. Furthermore, although there has been substantial progress on decarbonising the energy sector by developing renewable energy technologies, many of these technologies can only provide energy intermittently. They then need to be coupled with energy storage solutions in order to satisfy demand. Innovative energy storage solutions, such as Compressed Air Energy Storage (CAES), have been operational for many years, but on a relatively small scale. Solutions like this need to be developed urgently and at scale in order to keep up with the roll out of intermittent renewable energy technologies and satisfy energy demand fluctuations.

These solutions imply a renewed if not increasing usage of the subsurface. Indeed, the shallow crustal depths are not only where geo-energy reservoirs are located, it is also where large, high energy density storages can be engineered (Figure 1). The storage of fluids (compressed air, hydrogen and natural gas) within salt caverns proves to be one of the most promising underground storage options (Parkes *et al.* 2018; Caglayan *et al.* 2020 and references therein). Rock salt is highly soluble, impermeable to gas, and unless strain rates are very high, deforms by creep and flow rather than by brittle deformation formation or faulting (Parkes *et al.* 2018). In this context, understanding the response of rock salt to a broad range of (hydro/chemo-)thermo-mechanical loading scenarios is paramount for engineering design, operations, and potential associated risk management and mitigation. Such underground infrastructure could also provide a temporary storage solution for CO_2 that would add flexibility to a wide range of industrial clusters by introducing seasonal buffering capacity for delayed permanent storage or Power-to-X applications.

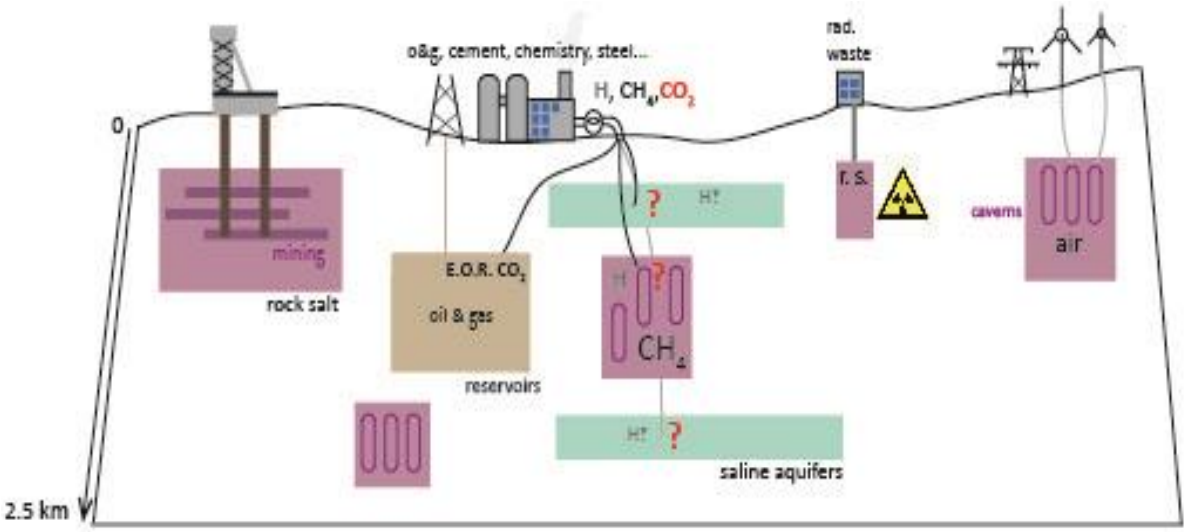

Figure 1 – Representation of the current and projected rock salt formations usage with respect to geological ore resources, storage and energy. Depth locations are indicative for a relative assessment. CO_2 storage potential in saline aquifers and rock salt caverns is suggested (in red) next to other on-going (in black) and projected (in grey) gas storage. E.O.R. = Enhanced Oil Recovery; CAES = Compressed Air Energy Storage.

1.1 Salt caverns

Salt caverns are artificial cavities created by solution mining in geological formations of rock salt (e.g., Bérest 2011): first, a well is drilled down into the formation, then water or undersaturated brine is injected through the completed well to dissolve the salt that is (mostly) extracted to the surface as brine (Figure 2). Cavern shape and the upward rise of the cavern roof is controlled by an inert fluid blanket pumped in and maintained at the top of the zone of active brine creation (Warren 2016). Residual brine volume that is not evacuated after leaching can occupy 30% of the total cavern volume (Panfilov 2016). The walls of the cavern are very resilient against reservoir degradation (Mokhatab *et al.* 2018). Early solution wells (1800's and extending into first half of last century) resulted in surface sinks, collapses and caved wells, which lead to early project abandonment. Today's rock salt caverns lifetime is in the order of tens of years.
Salt caverns are typically located at depths between 200 m and 2000 m, with an ideal depth for storage caverns is considered to be between 900 and 1700m because the limited flow of salt at that depth ensures the sealing property of the storage and a relatively small loss of storage volume with time (Cornet *et al.* 2018). At depths greater than 2,000 m ongoing salt creep tends to reduce cavern size (Warren 2016). The current deepest salt solution operation is in the Barradeel concession in northern Netherlands in Zechstein Z2 salts, which operates at approximately 2,800 m (Warren 2016).

The creation of such artificial underground cavities therefore disturbs the natural stress state of the rock salt formation and induces deviatoric (shear) stresses in the rock salt near the cavern (Mellegard & Dusterloh 2012); the highest magnitude being normally near the cavern walls and decreasing with distance into the geological formation. The range of pressures allowed in these caverns is assessed based on the onset of tensile stress and salt dilation at the cavern wall and is therefore dependent on the local conditions and use (Djizanne 2014; Cornet *et al.* 2018).

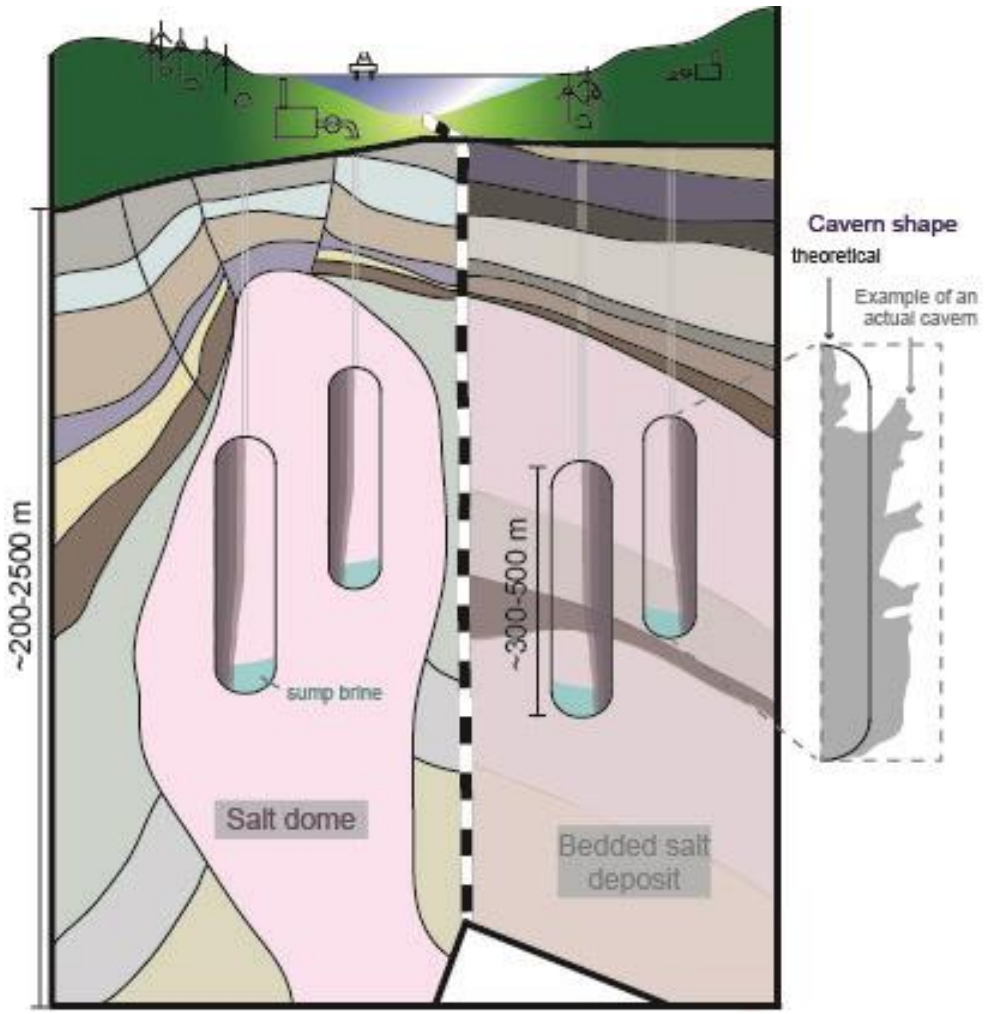

Figure 2 – Schematic to illustrate the depths of operational and proposed salt cavern systems in: a) salt domes/diapirs, and b) bedded salt formations. The insert on the right shows the common cylindrical shape used in modelling and illustration, versus an example of an actual cavern's shape (Huntorf NK1, Germany; after (Crotogino *et al.* 2001)).

Suitable rock salt formations for underground storage are found both in salt domes or diapirs, and massively bedded halite deposits (Figure 2). These formations are located in many regions worldwide with a noticeable greater concentration in Europe (Figure 3). Diapirs have the

advantage to be pure and homogeneous salt formations whereas bedded salt formations are more heterogeneous, notably due to the presence of mudstone and anhydrite interbeds. These interbeds can also have significant differences in terms of mechanical behaviour from rock salt, constituting weakness planes and offering potential for hydraulic fracturing area and leakages (Cosenza & Ghoreychi 1999; Cosenza *et al.* 1999; Minkley & Muhlbauer 2007). Although not all rock salt formations are suitable for energy or CO_2 storage, utilising only a small portion will be useful in solving energy intermittency issues and reducing CO_2 emissions.

1.2 Underground storage usage and potential

Due to the favourable physical properties of halite, salt caverns have been used for about sixty years for strategic underground oil and gas storage or to host products of the chemical industry on a large scale (Böttcher *et al.* 2017). Their high flexibility with regard to injection and withdrawal made them also highly suitable for short term, peak shaving operations. Indeed, with their much lower specific construction costs, a theoretically unlimited operating lifetime, a high level of protection from external influences (thanks to the several hundred meters thick overlying geological layers), large volumes (large gas cavern can hold more than 60 times the volume of a typical spherical gas tank) and high operating pressures, as well as a small surface footprint, they outrival surface gas tanks (Michalski *et al.* 2017).

They have therefore been used for Underground Gas Storage (UGS) and Compressed Air Energy Storage (CAES) as a solution to help meeting seasonal fluctuations in energy supply and demand by reducing peak load and increasing the supply security from the gas and electricity grids (Xing *et al.* 2015). Whilst UGS in depleted field storage dominates, market liberalisation has created a need for shorter-term storage allowing the growth of UGS in salt caverns in North America and Europe. In January 2013, 94 salt cavern facilities were in operation in the world, representing 14% of the total number of UGS sites (Judd & Pinchbeck 2016). Currently, there are three commercial CAES operating which are at: Huntorf (Germany, operational since 1978; Crotogino *et al.* 2001), McIntosh (USA, operational since 1991; Leith 2000), and Goderich, Ontario (Canada, operational since 2019; King *et al.* 2021). According to Evans *et al.* (2021), UK onshore and East Irish Sea areas offer very significant CAES exergy storage possibilities and capacity that, combined with renewable energy generation, could replace the current flexible power generation model at a national scale.

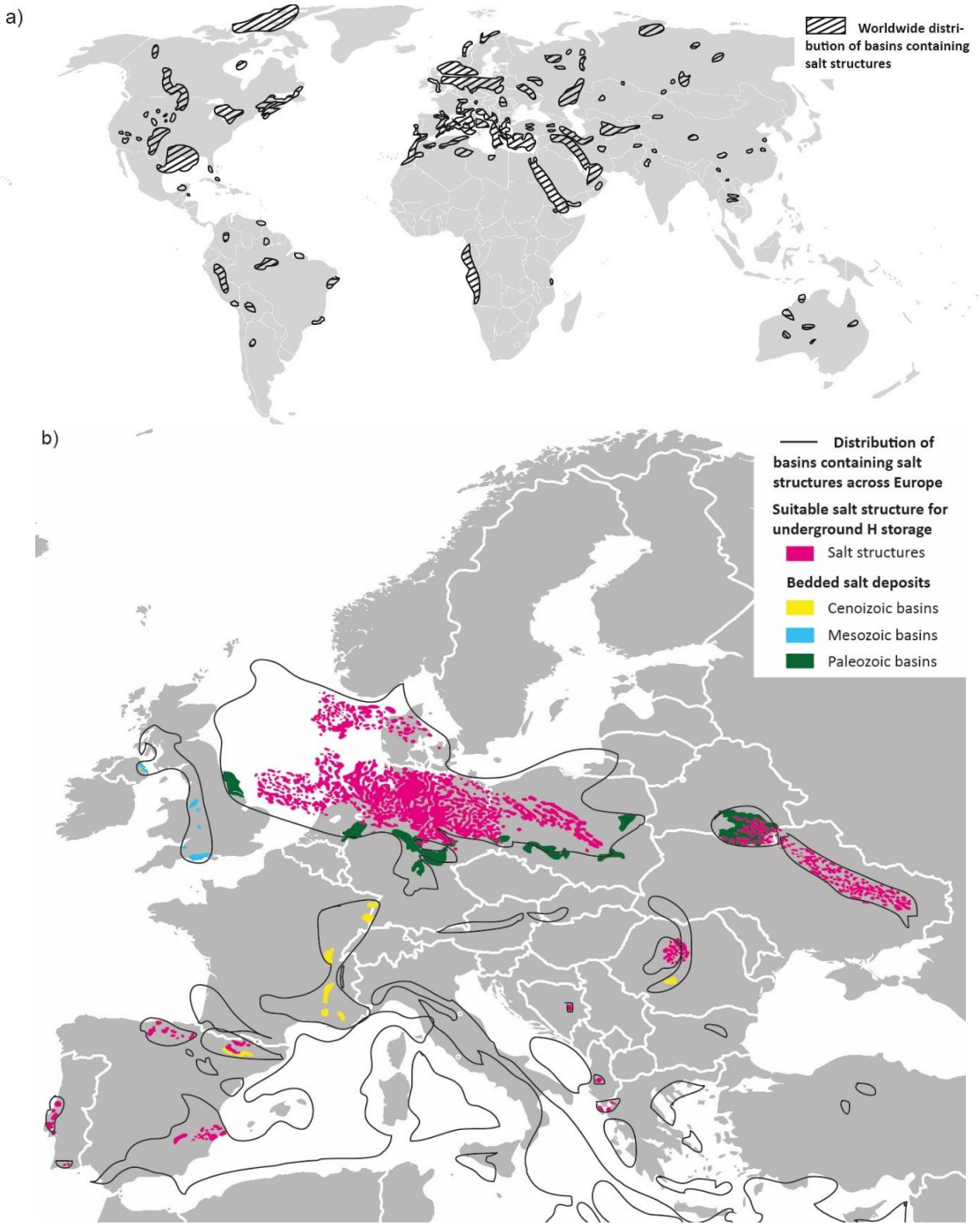

Figure 3 - Schematic distribution of the halite deposits worldwide (a), with greater details for Europe and Mediterranean Sea regions (b). After (Hudec & Jackson 2007; Donadei & Schneider 2016; Caglayan *et al.* 2020; Martin-Clave 2021); background maps: https://commons.wikimedia.org/wiki/File:BlankMap-World_gray.svg.

Despite early demonstration projects aiming at an introduction of hydrogen as a universal energy carrier in the 70s and 80s (e.g. the HySolar project; Steeb & Abaoud 1996), the Solar

Hydrogen Bavaria project (Szyszka 1990) and the Euro-Quebec Hydro-Hydrogen Pilot Project (Gretz *et al.* 1994), only few underground hydrogen storage caverns can be found around the world (at Teesside in England, in Germany, and Clemens Dome, Spindletop, Moss Bluff in the USA) (Landinger & Crotogino 2007; Tarkowski 2019). Those facilities were built notably for seasonal storage of hydrogen that is produced from nuclear power or associated with the production of oxygen (Forsberg 2006). However, geologic hydrogen storage is a relatively new technology compared to the experiences in natural gas or CAES. Recent studies and the pressing need to implement low carbon energy solutions have renewed the interest of UGS in salt caverns and the caverns' potential for large applications (Evans *et al.* 2011; Khaledi *et al.* 2016; Michalski *et al.* 2017; Caglayan *et al.* 2020).

For instance, 'blue' hydrogen – i.e. hydrogen produced from natural gas or steam-methane reformation –needs storage capacity for both hydrogen and the large volumes of CO_2 created in the process. Salt caverns connected to what is termed industrial clusters (i.e., geographical regions where energy supply and demand companies are co-located, often including a mix of heavy and light industries) appear to be a very suitable solution in that context, capable of storing temporary both hydrogen and CO_2 depending on the need and best techno-economical model. Caverns in the Lotsberg Salt (Alberta, Canada) have also been proposed as a serious option for temporary CO_2 storage (until a depleted gas reservoir becomes available for permanent storage), and for permanent CO_2 storage itself to cut down the emissions from the local, large-scale heavy oil and bitumen production sites (Dusseault *et al.* 2004). Such analysis reinforces the relevance of the storage potential of salt caverns as a technically viable solution for the reduction of anthropogenic CO_2 emissions into the atmosphere. With the European Commission net-zero greenhouse gas (GHG) emissions goal for 2050, with an intermediate target to reduce GHG emissions by at least 40% by 2030, compared to 1990 levels (European Commission 2021), there is a need to provide more details on the technical capacities of salt cavern storage and their relevance in a holistic European landscape, as it is done with the H2020 ConsenCUS project (https://consencus.eu/).

In particular, we need to further investigate and quantify the impact of shorter cycle times compared to strategic fossil fuel storage on the cavern stability. Whilst the creep behaviour of rock salt is well known, laboratory data and understanding on its thermo-mechanical (TM) brittle behaviour and upscaling model integrating these factors are scarce (Martin-Clave *et al.* 2021). Finally, in light of the multiple potential usages of the caverns, the TM impact of such multiple usage scenarios is also required.

In this study, we first summarise the existing knowledge on rock salt formation, mineralogy, and intrinsic properties, then focus on solution mined salt caverns, their current usages and typical

operational conditions. We then look in greater details on the thermo-mechanical behaviour of rock salt to identify where are the knowledge gaps and how to address them specifically in the context of UGS. We also discuss the potential of these structures to offer a temporary storage solution for CO_2 if integrated with high emitter industrial clusters prior to utilisation and/or permanent storage. The results aim to help framing where the next experimental testing and numerical modelling works should be to provide the data to inform appropriately policy and design.

2 Overall characterisation of rock salt

2.1 Precipitation and formation

Rock salt is an evaporite that consists either predominantly, or entirely, of halite, and forms from saline brine evaporation generally occurring in isolated water (lagoons), known as “primary deposits” (Figure 4). These lagoons are typically found in arid and warm climates, with water temperatures between 15 and 35°C (Gevantman *et al.* 1981; Jeremic 1994). Due to difference in solubility between different salt minerals, deposition occurs in facies where the most soluble salts are deposited at the end of the depositional process (Jeremic 1994). Different sequences of evaporites overlying and overlapping can occur as result of variations in topography, water depth and salinity due to the subsidence and sedimentary fillings of the basin.

The most accepted depositional model for bedded rock salt was first described by Ochsenius (1877) as the bar-basin theory: sea circulation is restricted by a natural barrier such as a sand bar, ridge or reef resulting in saltwater evaporation (Figure 4a). Periodic or low-rate continuous influxes of fresh (sea) water (by inlets or channels cutting across the barrier), rain and/or rivers, and evaporation, as well as a limitation of the outflow, lead to evaporite minerals precipitation into basin-wide beds (Figure 4a) (Ochsenius 1877; Gevantman *et al.* 1981; Melvin 1991; Jeremic 1994). The local temperature contrast of air and water, wind speed, humidity of the atmosphere and water surface turbulence control evaporation. If the rate of flow leaving the basin exceed the inflow, the system terminates (Melvin 1991). As illustrated in Figure 4b, rock salt is mainly deposited in marginal marine salinas above the sea level as a result of supratidal coastal sabkhas, distal margins of fan deltas and ephemeral stream deltas, and interdune

depressions (Melvin 1991). Some rock salt deposits, known as “secondary-cycle”, are also formed by a re-deposition of dissolved primary deposits.

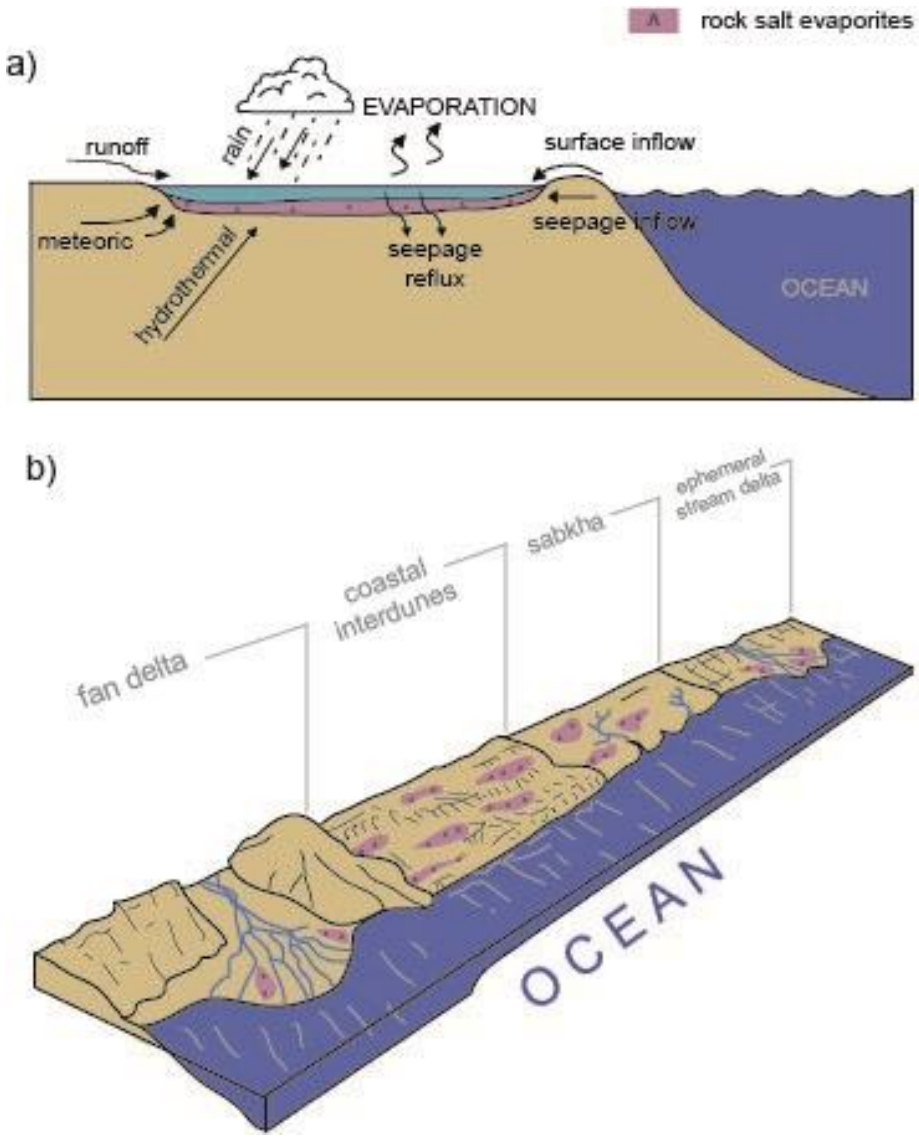

Figure 4: Rock salt deposits: a) model of evaporite formation, and b) marginal marine depositional environments where rock salt can be deposited. After Martin-Clave (2021) and Melvin (1991).

A notable process common in evaporites, including rock salt, is diapirism or halokinesis which is the spontaneous movement of material usually induced by the gravitational instability of the mass itself under the burden of a thick coverage of denser sediments (Giambastiani 2020). Diapirism is the term reserved for the penetration and rupture of the sedimentary cover phenomenon by ascending rock salt (Giambastiani 2020) (Figure 2). The halokinetic behaviour

of rock salt is due to its low density and high plasticity (creep), further facilitated by the high thermal conductivity, water content, deformability of the halite crystalline lattice, and the presence of K-Mg salts.

Evaporite deposits have been commonly formed in the Middle Cambrian, Permian, Jurassic or Miocene, and are buried all over the globe (Figure 3). Evaporite sediments have therefore been subjected to post-depositional mechanical alteration as folding and faulting structures, and also chemical alteration by water solution from water percolation in the evaporite rock formation. Other parameters like environmental depositional conditions, post-depositional changes may have affected the chemical composition of rock. As a result, not all salt formations may be suitable for UGS applications, and understanding the local geological history is crucial in assessing project viability.

2.2 Mineralogy

According to Jeremic (1994), four different saline facies can be distinguished for evaporites based on the chemical composition of the microstructure: i) calcium sulphate facies, ii) sodium salt facies, iii) chloride facies, and iv) potassium facies. Rock salt is primarily of the sodium salt facies and is composed mainly of halite (NaCl). It may also contain minerals from the other saline facies as well as other detrital material, in smaller quantities, such as dolomite, calcite, silts, sands clays, gypsum, anhydrite and polyhalite minerals (Gevantman *et al.* 1981; Jeremic 1994). It is thus a polycrystalline material formed mainly by grains of halite with a grain size range between less than 1 mm to several dm (Hunsche & Hampel 1999). Halite is colourless, and the natural colouration of rock salt is due to the inclusion of these other minerals as interstitial matter - impurities - and structural defects in the crystal lattice (Sonnenfeld, 1995). Rock salt formations are therefore heterogeneous at many scales which has implications on the variability of the physical and mechanical properties of the lithology (Liang *et al.* 2007; Wang *et al.* 2013).

2.3 Density, porosity and permeability

The density of rock salt is relatively low with an average of 2.17 g cm^{-3} at room temperature and it decreases with increasing temperature (1.90 g cm^{-3} at 801^{o}C, for example) and consequently depth. This is because of its near absence of porosity and the thermal expansion of the minerals - the volume increase exceeding the shrinkage due to the elevated confining pressure (Giambastiani 2020). Other examples of laboratory data of samples from a salt dome and a bedded formation by Gloyna & Reynolds (1961) recorded an average density of 2.139±0.20 g cm^{-3} and 2.153±0.01 g cm^{-3}, respectively.

Although widely acknowledged as one of the lowest permeability rocks, rock salt still naturally has a minute volume of connected porosity accessible to non-reactive fluids, that can become greater if accessed (and modified) by reactive fluids. Mechanical deformation due to changes in the environmental (confining) pressure can also induce modifications in the connected porosity (increase in micro-cracking for instance), impacting thus the global transport properties of the material. This is particularly of concern when the rock salt deformation transitions from non-dilatant to dilatant deformation at the so-called dilatancy boundary (Schulze *et al.* 2001). Another factor is the presence of impurities (usually anhydrite) that may create preferential pathways for fluid flow (Cosenza *et al.* 1999).

Several studies have investigated and reported on these properties; a summary of their findings with respect to gas as pore fluid is tabulated in Table 1. Note that oldest data exhibit higher values in comparison to the more recent ones; this is because the relaxation and disturbance from the mining operation that allowed the collection of the samples were not properly controlled (Gloyna & Reynolds 1961).

Table 1 – Summary of transport property laboratory measurements at room temperature in various rock salt samples.

Salt type	Formation/ origin	Pore fluid	Effective pressure (MPa)	Effective porosity (%)	Permeability (m^2)	Ref.	Notes
dome	Grand Saline, Texas, USA	He	[3.4;10.3]	1.71±0.54	[$9x10^{-15}$; $3.2x10^{-16}$]	Gloyna & Reynolds (1961)	Other fluids and permeabilities data available in the reference
bedded	Hutchinson, Kansas, USA	He	[3.4;10.3]	0.59±0.17	0 (<<10^{-19})	Gloyna & Reynolds (1961)	Other fluids and permeabilities data available in the reference
Synthe--tic	Ilarshaw Chemical Company	He	[3.4;10.3]	0	0	Gloyna & Reynolds (1961)	Other fluids and permeabilities data available in the reference
dome	Asse Speisesalz, Germany	Ar	[1;18.5]		[10^{-17}; 10^{-20}]	Peach (1991)	

bedded	Southeastern New Mexico, USA	unspecified	[2.4;18]		[10^{-16}; 10^{-20}]	Stormont & Daemen (1992)	
bedded	Amelie mine, Mulhouse basin, France	He	21	0.6	[$4x10^{-17}$ - 9×10^{-20}]	Cosenza et al., (1999) and references therein	Laboratory tests
dome	Gorleben Salt Dome, Germany	N_2	[5;30]		[$1.15x10^{-17}$; $3.32x10^{-20}$]	Popp et al., (2001)	

Overall, laboratory measurements on undisturbed rock salt samples are generally less than 10^{-20} m^2. Gloyna & Reynolds (1961) noted that the permeability tests involving the Grand Saline salt gave consistent values, although they were higher than permeabilities obtained using bedded salt. This difference appeared to be due to the greater relaxation accompanying the disturbance of the purer salt and the greater fragility of the larger crystals in the dome salt. However, deviatoric stresses significantly increases the permeability, as noted by Stormont & Daemen (1992; and references therein). Field measurements, performed on material exhibiting inherently more inhomogeneities than laboratory samples in rock composition or interlayers due to local disturbances, remained very small with values less than 10^{-18} m^2 (Berest *et al.* 1996; Stormont 1997; Cosenza *et al.* 1999).

2.4 Physical and mechanical properties

Halite has the highest thermal conductivity of sedimentary rocks (>6 W m^{-1} K^{-1} at 20°C; Yang *et al.* 2020), making saline masses some very effective heat conductors, deforming regional thermal gradients and significantly influencing the diagenetic reactions of the host rocks (Giambastiani 2020). Similar to its density, Morgan (1979) found that the thermal conductivity of rock salt also decreases with increasing temperature, from 4 W m^{-1} K^{-1} at 70°C to 2 W m^{-1} K^{-1} at 300°C.

Laboratory tests have reported elastic wave velocity measurements (V_P and V_S) of pure halite (natural and synthetic) and rock salt. Such measurements were performed following the ultrasonic pulse-transmission method (e.g. Birch 1960; Yin 1992; Vernik & Liu 1997). Compressional and shear waves were generated by means of lead zirconium titanate (PZT) piezoceramic transducers, with frequencies between 0.5 and 1.2 MHz. The values reported bracket the typical observed range for the material, with approximate values of V_P ~4400 m s^{-1}

and V_S ~2550 m s^{-1} commonly. Measurements for a range of rock salt samples are reported in Table 2.

Table 2 – Elastic velocities of pure halite and rock salt from laboratory measurements done at room P-T.

	Vp (m s^{-1})	Vs (m s^{-1})	References	Notes
Halite mineral	4500-4550	2590-2630	Mavko *et al.* (2009) and references therein	
Halite aggregate	4594	2624	Voronov & Grigor'ev (1971)	
Halite aggregate	4659 [7304]	2579 [3169]	Frankel *et al.* (1976)	[measurements in done at 2700 MPa]
Halite (Paradox member), USA	4400-6500		Tixier & Alger (1970)	
Goderich salt mine, Canada	4440-4750		Zong *et al.* (2017)	
Hockley salt dome, USA	4540±45	2690±40	Zong *et al.* (2017)	Range of measurement due to anisotropy
Bayou salt dome, USA	4540±45	2690±40	Zong *et al.* (2017)	
Zipaquirá Salt Mine, Colombia	3580±480	2100±320	Zong *et al.* (2017)	argillaceous rock salt
Gorleben Salt Dome, Germany	4284*-4575*	2523* -2659*	Popp *et al.* (2001)	*measured at 5-10 MPa of effective pressure
Rock salt	4400-6500		Leet & Birch (1942) and references therein	Measurements valid for halite, carnallite, sylvite
Jintan Salt Mine, Jiangsu Province, China	4000-4250	2050-2450	Li *et al.* (2018)	

Overall, both permeability and elastic wave velocities appear to be very sensitive to changes in rock salt microstructure, particularly through the formation or closure of microcracks (Popp *et al.* 2001). Rock salt is considered a weak rock, with low Unconfined Compressive Strength (UCS) and Young's modulus values, as summarised in Table 3. Very few data are available regarding its Point Load Index values.

Table 3 – Mechanical data for rock salt at laboratory room conditions. PLI = Point Load Index, UCS = Unconfined Compressive Strength, E = Young's modulus, ν = Poisson ratio.

	PLI (MPa)	UCS (MPa)	E (GPa)	ν	Ref.	Notes
Rock salt (tertiary)	1.5-1.9	23.6-32.4			Singh *et al.* (2012)	
Yingcheng salt deposit , China		17.06-20.27	4.4-5.9; 25.2*	0.31; 0.44*	Liang *et al.* (2007)	Bedded rock salt; *measured at a confining

						pressure of 15 MPa
Nevsehir-Gulsehir rock salt mine, Turkey		20.5-27.8**			Özkan *et al.* (2009)	**2.7:1 ratio
Mount Sedom, Israel			4.41-16.49	0.156-0.387	Hatzor & Heyman (1997)	
Khewra Mine (Nangaur-Nanganagar Basin), Pakistan		17.95-32.27	4.4-6.8		Singh *et al.* (2017)	
China?		30.12±4.32***	1.69±0.54***	0.213±0.22***	Yin *et al.* (2019)	***standard deviation
Jintan Salt Mine, Jiangsu Province, China		16.4-19.5				
Jiangsu Province, China		14.0	3		Liang *et al.* (2012)	Bedded salt
		15.6	2.27			After cyclic loading

2.5 Anisotropy

Rock salts may appear homogeneous and isotropic, particularly if consisting of pure halite, but they are best described as inherently anisotropic on all scales, mostly due to their well-developed bedding planes (Djahanguiri & Matthews 1983) and preferred orientation of halite crystals (Carter & Hansen 1983). Yet, the effect of anisotropy on strength, deformation and elastic parameters in this rock type has been largely overlooked, with models assuming, for instance, that micro-crack propagation and healing lead to isotropic stiffness changes. Hatzor & Heyman (1997) first reported in their study that the initiation of inelastic deformation (dilation) and relative volume growth are highly sensitive to anisotropy. The stress at onset of dilation depends on the orientation of the discontinuities: maximum stresses are measured when compression is normal to bedding planes and minimum values are measured when compression is parallel to bedding planes. Therefore, they proposed a new, empirical model for dilation in anisotropic rock salt, calibrated using their specific data set of Mount Sedom samples.

The elastic anisotropy and its impact on seismic data interpretation in rock salt had also been highlighted by Raymer *et al.* (2000), as they quantified plausible high levels of seismic anisotropy (5% P-wave anisotropy and 10% shear-wave splitting) from the effective elastic

constants for the modelled polycrystalline aggregates. Yet it is only recently that Prasse *et al.* (2020) presented unambiguous evidence that the Mahogany salt body, located in the Northern part of the Gulf of Mexico, is seismically anisotropic. Working at a smaller scale, Shen *et al.* (2020) demonstrated experimentally in synthetic samples that rock salt develops brittle (crack) damage-induced anisotropy.

3 Thermo-mechanical behaviour

Rocks are three-phase systems where minerals, pores and microcracks (filled or not), density, moisture content, degree of saturation, absolute and effective porosity, hardness of the minerals, grain size, microcracks, mineralogy, and so on, can influence the strength and deformability of rocks and rock masses (Giambastiani 2020). Rock salt is no different, yet it does exhibit a distinctive behaviour compared to any other rocks. Indeed, rock salt is renowned for deforming under pure creep even at low pressure and (room) temperature, where irreversible deformation (plastic) take place without fracture development. And it can also host brittle deformation related to crack formation (Hunsche & Hampel 1999).

Rock salt can deform by two stress-dependent domains as described by Van Sambeek *et al.* (1993) and Cristescu & Hunsche (1998), with the i) dilatancy domain and ii) compaction domain, separated by the dilatancy-compaction boundary that depends on the loading geometry, or internal microstructure from natural deformation and sedimentary processes (Covey-Crump *et al.* 2016), and rock salt lithology (Schulze *et al.* 2001). As summarised by Martin-Clave (2021), when the state of stress stays in the dilatancy domain, the deformation of rock salt is driven by micro-crack formation and propagation resulting in an increase of the porosity and creep failure, mechanical weakening and acoustic emissions. In the non-dilatant compaction domain, plastic deformation and compaction of micro-cracks can lead into a healing process and closure of fractures with a decrease of permeability. Pure creep as result of dislocation movement and elastic deformation is also observed in the non-dilatant compaction domain (Hunsche & Hampel 1999; Schulze *et al.* 2001). Creep in rock salt can also be affected by external factors such as temperature and stress as well as the intrinsic structure, water content and second phase content (Günther *et al.* 2015).

Schulze *et al.* (2001) note that damage and deformation-induced crack density in rock salt is strongly controlled by confining pressure (Figure 5). Rock salt strength and plasticity increase with increasing confining pressure. When the stress state stays below the dilatancy domain, failure occurs gradually, not spontaneously. Beyond the dilatancy boundary, a decrease in rock strength and strain hardening can occur as result of accumulating micro-damage during loading. In the non-dilatant compaction domain, plastic deformation and steady state creep are steady under effective stress (Schulze *et al.* 2001). Pore pressure increase as result of permeation of fluids may also develop and lead to a reduction of the confining effect of lithostatic pressure (effective pressure) resulting in fracturing damage and dilatancy (Schulze *et al.* 2001). Interestingly, brittle damage is likely to be repaired by subsequent ductile flow arising from crystal plastic deformation and pressure solution processes. However, this process, and in particular the timescales and conditions that lead to this process occurring, are not well understood.

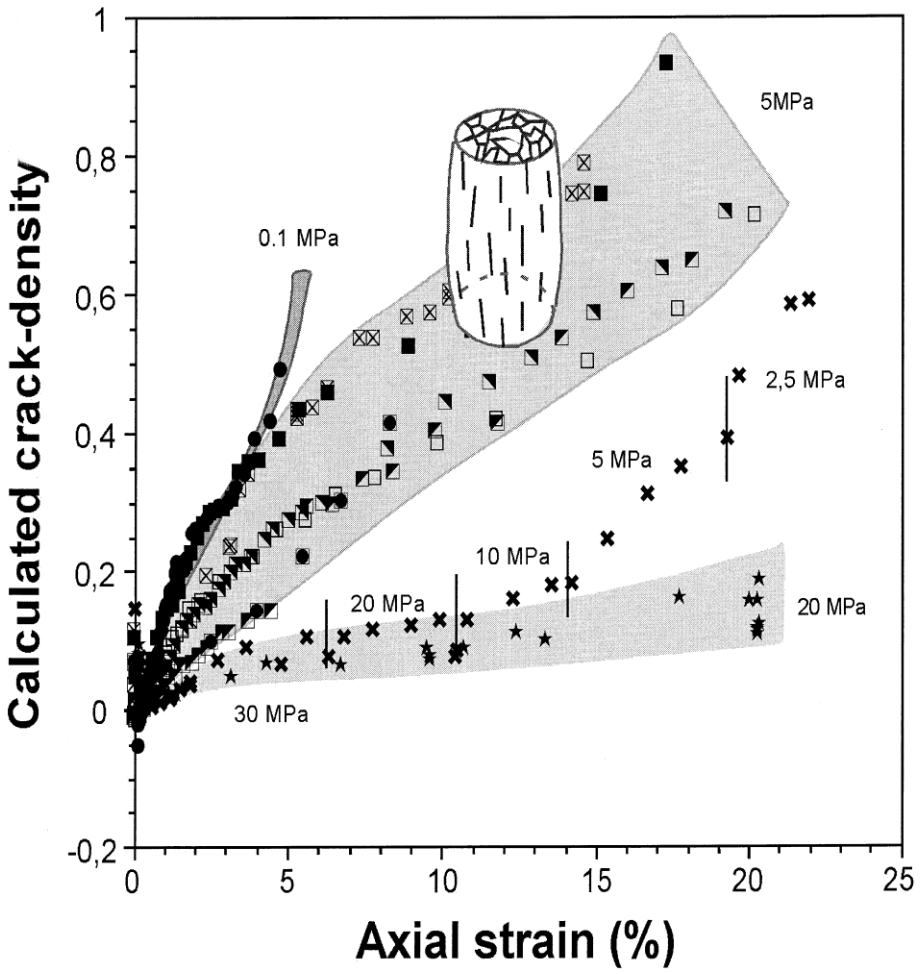

Figure 5 - Dependence of the calculated crack density on confining pressure during deformation in compression in rock salt (Schulze *et al.* 2001).

Rock salt deformation is equally if not even more sensitive to temperature. Indeed, the stiffness of rock salt decreases with the increase of temperature (Senseny *et al.* 1992) at a rate of

$$-0.04 \leq \frac{\partial E}{\partial T} \leq -0.016 \ GPa/K$$

where E is the Young's modulus, and the temperature T is expressed in Kelvin (K).

Four mechanisms controlling deformation in rock salt have been identified for constitutive models with imposed stress or temperature (Munson 1979; Bérest 2019) (Figure 6):
1) defect-less flow at extremely high stresses;
2) dislocation glide controlling quasi-static stress-strain tests;
3) dislocation climb;
4) diffusion creep controlling creep in two variations - Nabarro-Herring creep by volume diffusion material transport and Coble creep by grain boundary material transport;
The two main deformation mechanisms for plastic deformation are:
i) dislocation creep, which is the result of dislocations moving through the material,
ii) pressure-solution (solution-precipitation) creep, which is a stress-driven mass transfer process (Spiers *et al.* 1990; Urai *et al.* 2008).

Experimental data from Carter *et al.* (1993) and Schenk & Urai (2004) also show that wet rock salt can show deformation by dislocation creep with “fluid-assisted" dynamic recrystallisation processes at low temperatures, and variations in temperature can lead to thermoelastic strains within the crystal lattice (Berest *et al.* 2005). At low temperature (room temperature) and low deviatoric stress, the domain that encompasses the domain of interest for designing salt caverns notably, plastic deformation appears to be mainly driven by microcracking and brittle rheological behaviour (Peach *et al.* 2001; Popp *et al.* 2001). The micromechanisms controlling creep in this domain (5th in Figure 6) are still not fully understood; pure empirical data are used to extrapolate rheological behaviour in this domain (Bérest 2019).

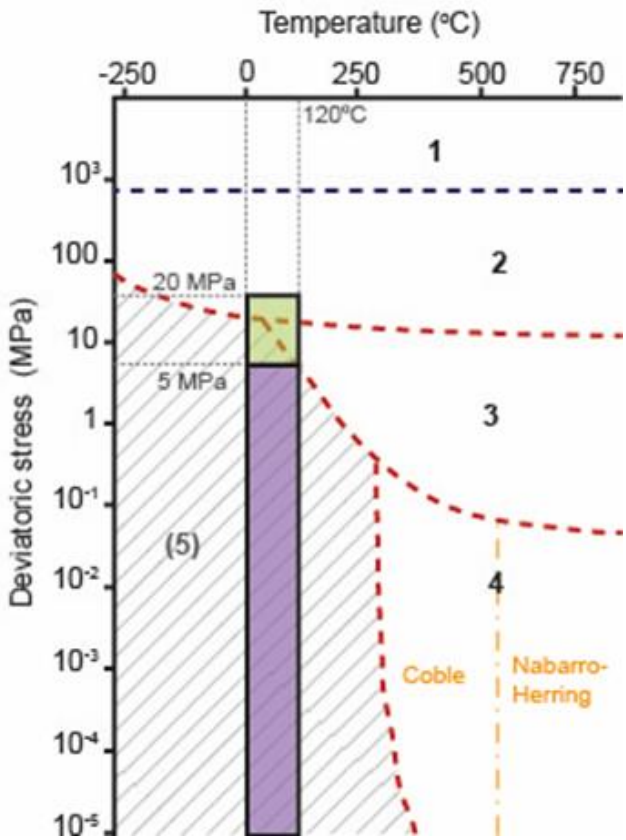

Figure 6 – Simplified deformation mechanisms map: 1) defect-less flow, 2) dislocation glide, 3) dislocation climb, and 4) the two variations of diffusion creep - Nabarro-Herring creep by volume diffusion material transport and Coble creep by grain boundary material transport. The grey hatched area indicates the domain where plastic deformation appears to be mainly driven by microcracking and brittle rheological behaviour. The green area brackets the typical laboratory experimental conditions, and the purple one the domain of interest for designing caverns and mines. After Martin-Clave (2021) and references therein.

4 Reservoir scale considerations for salt caverns

Although extensive work has been carried out to characterise and understand the physical properties of salt at a lab scale, it is important to consider the specific operational parameters related to UGS to be able to determine safe operational working conditions. Note that UGS here includes the storage of any gas in the subsurface within a salt cavern (e.g., air, natural gas,

CO_2, H...). Below we discuss some of the most important considerations when moving to the reservoir scale.

4.1 Thermally induced stresses

Berest (2019) gives a thorough review of how and why temperature changes occur within salt caverns used for fluid storage (gas and liquid). Here we focus on the mechanisms most likely to give rise to thermal stresses in the cavern walls which may ultimately lead to stability and integrity issues. For a broader overview of temperature related processes in salt caverns we direct the reader to Berest (2019).

Thermal stresses are induced in the cavern walls through the cyclic injection and production of gas, where the magnitude of the induced stress is dependent on the temperature difference between the gas and the host rock. Although this can be affected by many things (such as the temperature the gas is injected at), two of the main considerations are the gas injection/withdrawal rate and the shape of the salt cavern (Leuger *et al.* 2012).
While rock salt usually deforms in a ductile manner, under certain circumstances brittle deformation will occur through the formation of fractures. In the case of UGS in salt caverns, induced thermal stresses may lead to tensile fracturing in the cavern walls. This can lead to leakage pathways for gas to migrate but also cavern stability and integrity issues.

Recent studies (Bérest 2011, 2019; Böttcher *et al.* 2017) have shown that more frequent cycles of gas injection/withdrawal lead to greater differences in temperature between the host rock and the gas. If gas injection/withdrawal rate are extremely rapid, then the system may be approximated as adiabatic (i.e., that heat is not transferred from the gas to the host rock and vice versa). For an adiabatic system temperature contrasts between the gas and the host rock are the greatest, and therefore thermally induced stresses will also be largest. For a more transient system, where the heat is transferred between the gas and the host rock the thermal gradient and consequently induced thermal stresses will be less. While it has been shown that a truly adiabatic system is unlikely (Nieland 2008; Bérest 2011), reducing the frequency of gas injection/withdrawal cycles has been demonstrated to lead to a decrease in the cavern wall temperature flux over time (Böttcher *et al.* 2017) (Figure 7). This therefore leads to a smaller temperature contrast between the gas and the host rock and lower thermally induced stresses. Böttcher *et al.* (2017) also investigated the possibility of pausing operations for some time to see if tensile stresses in the cavern wall would be reduced over time but found that when operations re-started those tensile stresses would be induced again soon after.

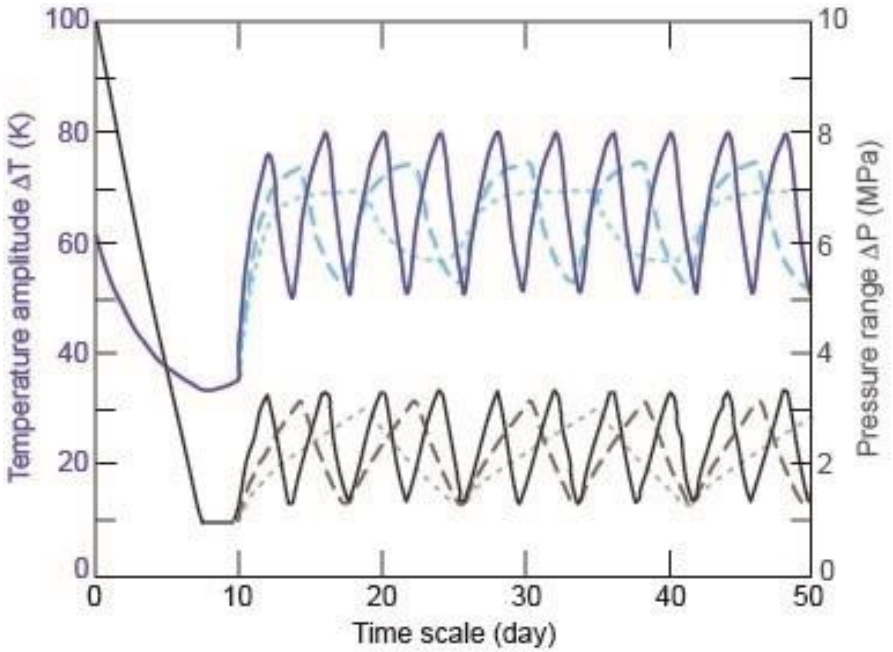

Figure 7: Example of pressure and temperature boundary conditions at the wall of a salt cavern zeroed here at the start of cyclic loading. Three time series for operational cycles of 4-days (solid line), 8-days (dashed line) and 16-days (dash-dotted line), respectively. Modified after Böttcher *et al.* (2017).

While the depth of penetration of thermally induced stresses is dependent on specific operational practices, under normal circumstances it is generally considered to be a very local, thin, "skin" effect within the cavern wall i.e., on the cm scale, (Bérest 2011; Böttcher *et al.* 2017). Although the effects are local and are not likely to penetrate deep into the host rock, they are still important to consider as they can lead to cavern stability and integrity issues.

The effect of thermally induced stresses during a sudden and full escape of gas (blowout) was investigated by Sicsic & Bérest (2014). In their analysis they investigated how a sudden drop in temperature (between 40 - 78°C) may damage a salt cavern wall, using the Moss Bluff natural gas storage facility in Texas as a basis for their model. In 2004 this facility indeed experienced a blowout, which lasted several days and resulted in a sudden and total loss of gas. The models of Sicsic & Bérest (2014) demonstrate that under the blowout conditions severe damage may accumulate in the cavern walls (Figures 8 and 9).

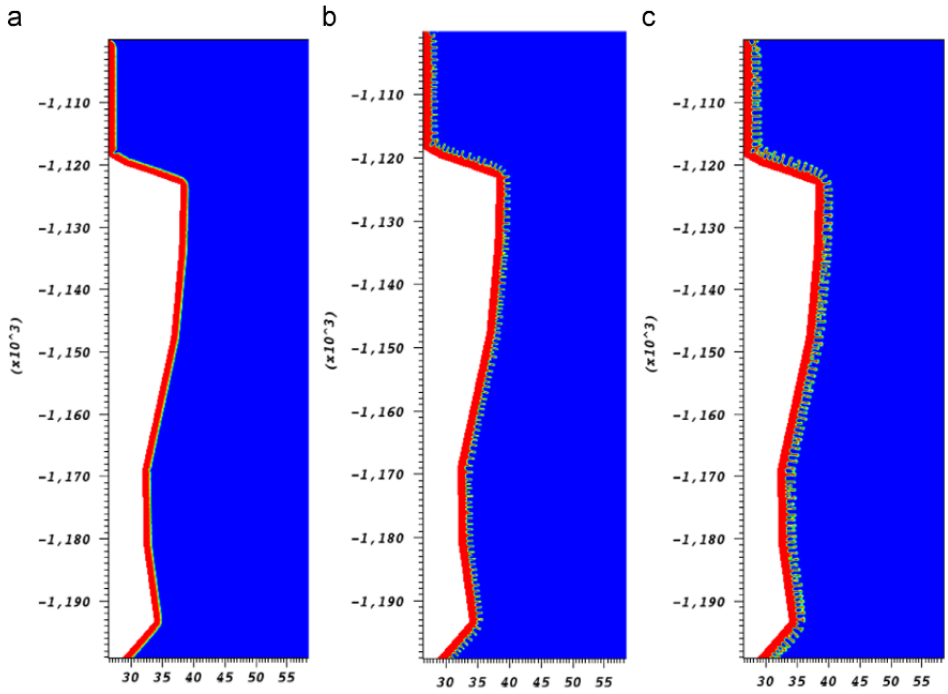

Figure 8: Damage field after a blowout in a salt cavern (distance in meters): severe thermal shock caused by a drop in temperature of 78°C over 7 days (c), with snapshots at (a) 1 day and (b) 3 days. Blue denotes the intact material, and red denotes the totally damaged material. In these conditions, extensive damage is observed on the cavern's walls with little deep penetration into the host rock. From Sicsic & Bérest (2014).

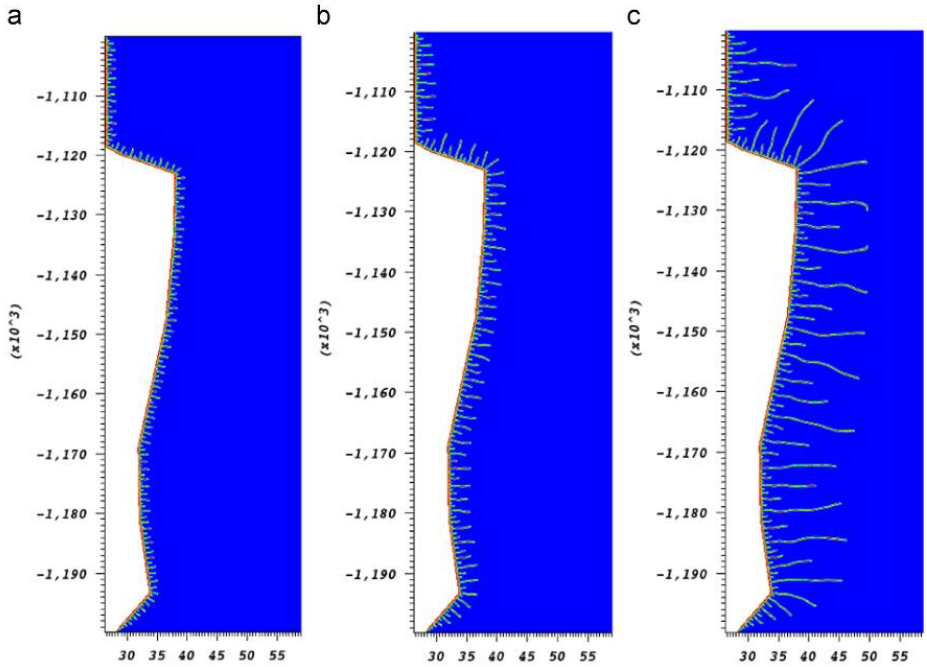

Figure 9: Damage field after a blowout in a salt cavern (distance in meters): mild thermal shock caused by a drop in temperature of 40°C over 7 days (c), with snapshots at (a) 1 day and (b) 3 days. Blue denotes the intact material, and red denotes the totally damaged material. In these conditions, a series of longer individual fractures form along the cavern wall and penetrate deep into the host rock From Sicsic & Bérest (2014).

While Sicsic & Bérest (2014) admit that there are some simplifications to their model, conceptually it is useful as it demonstrates that 1) damage in the cavern walls can extend tens of metres into the host rock as a result of a blowout, 2) smaller temperature drops will lead to individual fractures penetrating the cavern wall, while more significant temperature drops will lead to more widespread damage, but shallower penetration of individual fractures. Widespread damage is likely to cause stability issues and spalling, while deeper penetrating fractures have the potential to become leakage pathways for gas migration. Although these kind of drops in temperature are only likely during an accident, it demonstrates that it is important to consider the effect of thermally induced damage when designing operational constraints. This is particularly true for salt caverns, where given the low tensile strength of salt (1-2 MPa, (Fuenkajorn & Phueakphum 2010, 2011; Gudmundsson 2011) a temperature difference of only a few degrees Celsius may lead to tensile fracturing.

The cavern shape is also important to consider when analysing thermally induced stresses. For example, for the same volume (gas capacity) a spherical cavern will have a smaller surface area in comparison to an elongated cylindrical cavern. In practice this means that temperature between the gas and the host rock is more easily distributed, and so thermally induced stresses are less (Böttcher *et al.* 2017). However, caverns are unlikely to be ideal spheres or cylinders and will have much more complex geometries (as illustrated in Figure 2), which will perturb the in-situ and induced stresses (Sicsic & Bérest 2014; Bérest 2019). Furthermore, although thermal stresses may be less for a more elongated cavern shape, the mechanical stresses induced at the cavern ends may be more for a cavern with a larger aspect ratio (Gudmundsson 2011).

Another major uncertainty concerns the long-term pressure evolution of the fluid trapped in the cavern (Cornet *et al.* 2018). Thermal expansion of the brine due to temperature increase (Bérest & Brouard 2014) coupled with the volume loss due to cavity closure increases cavern pressure (Berest *et al.* 2001) while counteracting processes like gas leakage (Huang & Xiong 2011) and fluid permeation through the salt may also operate. Finally, it is worth noting that thermal convection can be induced by the temperature gradient in the caverns whose height can be of several hundred meters (Bérest 2019).

4.2 Cavern closure

Given the viscous nature of rock salt over geological timescales, it is often assumed that the state of stress in salt is isotropic (with the principales stresses $\sigma_1 = \sigma_2 = \sigma_3$) (Dusseault *et al.* 2004). However, through the creation of a cavern the stresses locally are perturbed, and unless the cavern pressure is maintained at a value equal to the lithostatic stress, deviatoric stresses will be introduced. Depending on local stress conditions deviatoric stresses can lead to cavern closure (or convergence) through creep, or brittle failure through tensile fracturing, where both processes occur over engineering timescales.

It is difficult to measure cavern closure directly, as the resolution of the tools used for this purpose (e.g. sonar, lasers) is too low to measure the small changes of volume (Cornet *et al.* 2018). However, Brouard *et al.* (2013) measured the closure of an abandoned salt cavern indirectly through measuring both the pressure at the wellhead and the outflow rate of brine over time and relating it to a change in cavern volume. They found that the closure rate of this particular salt cavern was 0.001% per year (10^{-5} per year). Cornet *et al.* (2018) considers a 10% closure to be a critical limit from an engineering perspective, and so at a rate of 0.001% it would take 10,000 years to reach a closure of 10%. While the data from Brouard *et al.* (2013) provide data from a real, full-scale cavern, they are from a cavern that had been idle for almost 30 years. It is known that the closure rate decreases over time, as the cavern pressure tends towards the lithostatic stress (Dusseault *et al.* 2004), and therefore initial closure rates may have been higher than those calculated by Brouard *et al.* (2013). Furthermore, the closure rates for an idle, abandoned cavern are likely to be different to those of an operational UGS. For an operational UGS, both direct and indirect measurements of cavern closure are extremely difficult, and therefore numerical methods must be used instead.

Khaledi *et al.* (2016) carried out analysis of the volume loss of a cavern with a depth to top of 325m, under two operational scenarios. The first with a minimum and maximum pressure of 3 and 8 MPa respectively (5.5 MPa mean pressure), and the second with a minimum and maximum pressure of 7 and 12 MPa respectively (9.5 MPa mean pressure). Their model also included an overburden stress of 10 MPa, and the results of the model are plotted in Figure 10. Cavern closure was greater for the first scenario, where the mean cavern pressure was lowest. Again, this is because the closure rate is dependent on the difference between lithostatic stress and cavern pressure. For the second scenario the closure rate is near constant, but in this scenario the difference between the lithostatic and mean cavern pressure is 0.5 MPa. For both scenarios the total closure over the time analysed is low, but the closure rate is between 0.04 per year and 0.8 % per year which is higher than that measured by Brouard *et al.* (2013).

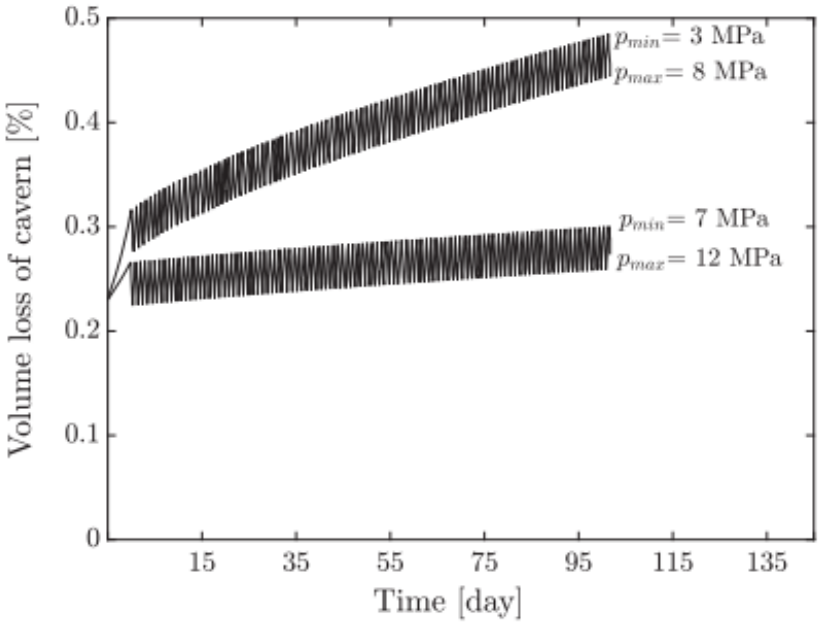

Figure 10: Volume loss of a cavern (VL) for two loading scenarios, taken directly from Khaledi *et al.* (2016).

One potential reason for this discrepancy may be because the measurements of Brouard *et al.* (2013) are from a brine filled cavern that has been idle for 30 years, during which the cavern may well have been closing, and the cavern pressure will have increased thus reducing the effective pressure (i.e., the difference between the lithostatic pressure and the cavern's pressure), and consequently the closure rate. Compare this to the analysis of Khaledi *et al.* (2016) where cavern closure is calculated from the start of operations. For an operational UGS, the cavern pressure will be maintained between the set limits, rather than allowing it to increase over time – as is the case for an abandoned cavern – and as such the effective pressure will be kept constant. This in theory would lead to a constant closure rate, rather than one that decreases over time. For the closure rates deduced from Khaledi *et al.* (2016) this would mean the cavern would reach of volume loss of 10% within 12.5 – 250 years, which is within the normal target lifetime of a salt cavern. While closure rates are also dependent on other parameters which are project specific (e.g., cavern depth, size, shape, host rock grain size) this stresses the importance of making sure that the correct pressure limits are set in order to maximise the operational lifetime of a cavern. For reference, a list of operating pressures for a number of UGS sites is provided in Table 4; simplified from Martin-Clave (2021).

Table 4: Details of existing UGS sites, including operating pressures.

Location	Type of storage	Operating Pressure (MPa)	Depth (m)	Reference
Huntorf, Germany	CAES	3.3 - 7	725	Landinger *et al.* (2013)

Mcintosh, USA	CAES	4.5 - 7.6	450	He *et al.* (2017)
Teesside, UK	Hydrogen	4.5	370	Kruck *et al.* (2013)
Clemens, USA	Hydrogen	7 – 13.5	930	Kruck *et al.* (2013)
Moss Bluff, USA	Hydrogen	5.5 - 15.2	822	Kruck *et al.* (2013)

4.3 Fatigue from cyclic loading

As discussed in the sections above, deformation of rock salt under static or continuous loading is already complex, however for the purposes of UGS the effects of cyclic loading need to also be considered. As long as the gas pressure conditions do not induce stresses that overcome the host rock's strength, the main extra consideration is that of damage caused by fatigue. Fatigue failure occurs when the strain energy exceeds a critical energy level equivalent to failure under non-cyclic loading (Ma *et al.* 2013; Khaledi *et al.* 2016). Damage, which is the result of fatigue failure, may only occur when the host rock is in the dilatancy regime (as opposed to the compressional regime), whereby microcracks open up (Khaledi *et al.* 2016). Crucially, the onset of dilatancy is a precursor to macroscopic failure, rather than macroscopic failure itself.

Operating at low cavern pressures gives the greatest risk for fatigue and failure as this gives rise to a higher effective pressure (Khaledi *et al.* 2016). Khaledi *et al.* (2016) model the damage caused by cyclic loading for two different loading scenarios, one where the maximum effective pressure was 7 MPa (mean effective pressure of 4.5 MPa) and the other where the maximum effective pressure was 3 MPa (mean effective pressure of 0.5 MPa). They use a Long-term Failure Ratio (LFR) criterion to establish when permanent damage would occur, where positive values indicate areas that incur damage (Figure 11). Interestingly, they demonstrate that for the scenario where the effective pressure is highest, damages occur during the initial filling phase i.e., when the cavern pressure is reduced to its minimum for the first time, and before any cycling loading has started. After 100 cycles, the amount of damage has increased and this corresponds to a significant increase in host rock permeability (Figure 12).

The numerical example presented by Khaledi *et al.* (2016) demonstrates that the internal pressure of the cavern during the cyclic loading operation should be set in a way that the stresses around the cavern remain below the dilatancy boundary. Otherwise, micro-cracking

and damage propagation may result in fatigue failure, and consequently a potential decrease in cavern stability and increase in host rock permeability.

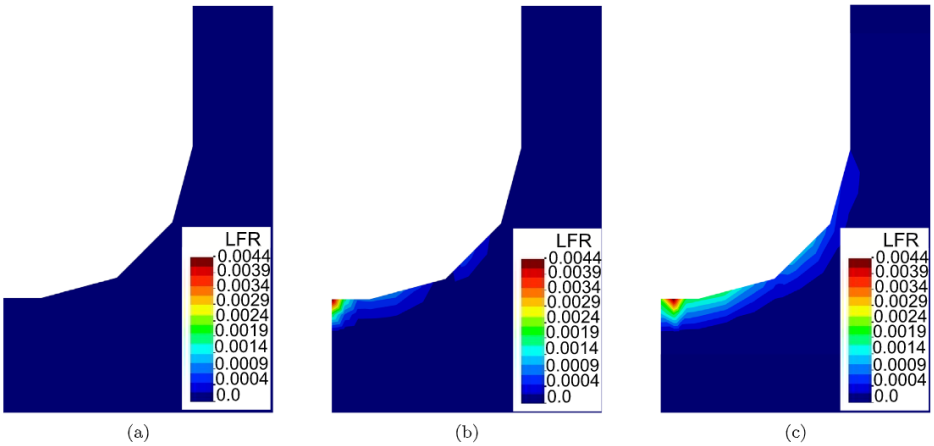

Figure 11: Contour plot of long-term failure ratio (LFR) for (a) Min pressure = 7 MPa, Max pressure = 12 MPa, after 100 cycles (b) Min pressure = 3 MPa, Max pressure = 8 MPa, after at the end of first filling phase (c) Min pressure = 3 MPa, Max pressure = 8 MPa, after 100 cycles. From Khaledi *et al.* (2016).

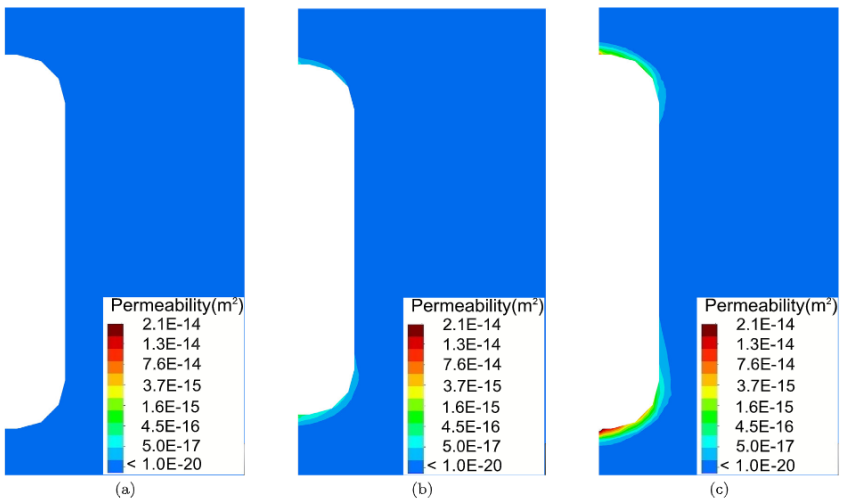

Figure 12: Contour plot of permeability around the cavern for (a) Min pressure = 7 MPa, Max pressure = 12 MPa, after 100 cycles (b) Min pressure = 3 MPa, Max pressure = 8 MPa, after at the end of first filling phase (c) Min pressure = 3 MPa, Max pressure = 8 MPa, after 100 cycles. From Khaledi *et al.* (2016).

The models of Khaledi *et al.* (2016) are of a cavern with a simplified boudin like geometry, with smooth edges and spherical top and bottom. As such, the damage criterion, LTF, is only exceeded at the top and bottom of the cavern. In reality, cavern geometry will be much more

complex with cavern walls that are not smooth (see Figure 2). In such circumstances “sharp edges” will cause local stress concentrations in the cavern wall, which may ultimately lead to damage.

5 Concluding remarks and future research directions

Understanding the thermomechanical behaviour of rock salt, from grain to reservoir scale, is fundamental for the accurate assessment of UGS in salt caverns, be it for permanent storage of CO_2, seasonal gas storage, or temporary storage of hydrogen, compressed air or CO_2. Each of these applications operate on a different temporal scale, and consequently this means that the specific project needs need to be taken into account during design, development and operation.

We have collated and reviewed a large body of literature covering the different temporal and spatial scales that are important for the use of salt caverns for UGS, from rock salt formation and grain scale mechanics, to the reservoir scale and operational considerations. At the reservoir scale our focus has been on a more frequent cycling of gas, which is more relevant to energy storage (hydrogen and compressed air) and temporary storage of CO_2, rather than the seasonal storage of natural gas and permanent storage of CO_2.

Due to the pressing need to reduce CO_2 emissions, the rapid development of intermittent renewable energy technologies has led to a challenge in matching energy supply and demand, which will only become more difficult as the energy transition continues. Energy storage in the subsurface offers a unique and pragmatic solution, where at times of high supply and low demand energy can be converted and stored in the subsurface using either hydrogen or compressed air as an energy carrier. Then at times of low supply the stored energy can be converted to satisfy periods of high demand.

Salt caverns have been used for many used to store a variety of fluids, and as such many of the processes fundamental to storage operations are well-understood. Nevertheless, knowledge gaps still exist, particularly for operations with a more frequent cycling of gas. We highlight some of these knowledge gaps below, and offer some suggestions on how to address these using laboratory experiments.

5.1 Permeability evolution of rock salt under cyclic loading

One of the main concerns resulting from cavern wall damage is that the permeability of the host rock increases and fluids can then escape to the surrounding formations. Salt rock is usually considered impermeable on engineering timescales, but under certain conditions brittle failure(s) can lead to an increase in permeability (Khaledi *et al.* 2016). Although this has been analysed using numerical methods, there is a lack of experimental data addressing this question specifically. To date much of the experimental data that exists on cyclically loading samples of rock salt focuses on the effects on mechanical properties, rather than permeability (Fuenkajorn & Phueakphum 2010; Ma *et al.* 2013; Fan *et al.* 2016; Martin-Clave *et al.* 2021). Although it may be argued that the evolution of mechanical properties may be a proxy for the evolution of permeability, to our knowledge this has not be explicitly measured and quantified. Those that do also measure permeability (Peach 1991; Fuenkajorn & Phueakphum 2011; Chen *et al.* 2020) usually do so under static loading conditions, and do not replicate the high frequency loading conditions that occur in UGS applications.

As such we would propose that the permeability of samples of rock salt are measured during cyclic loading experiments, under realistic UGS operational conditions (see Table 4). In addition, we believe it would also be useful to continuously measure ultrasonic wave velocities (which can then be used to determine the elastic moduli) and record acoustic emissions data (which can be used as a proxy for crack formation, and therefore damage). This would then help improve our understanding between fatigue cracking, and its effects on rock salt permeability and mechanical properties.

5.2 Healing potential of rock salt by changing stress regime

Given the potential negative effects caused through damage it is important to understand under what conditions healing of fractures may occur in rock salt, and how this may improve the stability and integrity of caverns during operations and abandonment. Although the healing potential of rock salt is often considered to be a significant driver for developing salt caverns for geo-energy applications, experimental data on the healing process is sparce.

Peach (1991) conducted permeability experiments on deformed samples of Asse salt under both dry (using Argon as a permeating fluid) and saturated (using brine as a permeating fluid) conditions. They found that for both conditions the sample permeability decreased with increasing effective pressure, but that the permeability decay was greater under wet conditions. Under dry conditions the permeability decay could be explained by an elastic crack closure model (Walsh 1981), but that for wet conditions an enhanced decay of permeability was likely

due a crack healing process, possibly via a process of re-crystallisation of minerals. Chen *et al.* (2020) came to a similar conclusion that the presence of brine enhanced the healing of rock salt under their experimental conditions, and that the presence of oil hindered any healing of fractures. Although both of these investigate the potential for crack healing under subsurface conditions, they both involve the presence of brine, which for UGS operations will only exist in the sump and therefore will unlikely contribute significantly to any healing process.

Fuenkajorn & Phueakphum (2011) measured the permeability of samples containing macroscopic discontinuities (fractures and saw cuts) for dry samples, using nitrogen as permeating fluid. Their research showed that between subsequent loading cycles the sample permeability decreased, which they attributed to the potential healing of fractures. However, they also acknowledge that they did not investigate how the fracture roughness changed between cycles. It could be that the asperities on the fracture surfaces (which keep the fracture open) deform between successive increases in confining pressure, leading to a decrease in fracture aperture and consequently a decrease in permeability. Although this mechanism may also be important during the operation of UGS in salt caverns, it may be subtly different to a healing mechanism that operates through pressure solution for example. Fuenkajorn & Phueakphum (2011) only investigated how macroscopic discontinuities may respond to mechanical loading. While this may be important to consider in UGS applications, it is likely that the precursor to macroscopic failure will be damage caused by the formation of microcracks, which ultimately lead to macroscopic failure. As such, we stress that future work should focus on understanding how the healing of microcracks may occur through mechanical loading, and in the absence of brine.

5.3 The impact of thermal induced damage

While the risk of thermally induced damage in salt caverns used for UGS is well recognised, most research to date has focused on the reservoir scale using analytical and numerical methods (Bérest 2011, 2019; Leuger *et al.* 2012; Sicsic & Bérest 2014; Böttcher *et al.* 2017) empirical data from abandoned salt mines (Staudtmeister *et al.* 2017) and in-situ experiments on large salt masses (Ngo & Pellet 2018). There therefore is a lack of experimental analysis investigating the micro and meso scale processes governing thermally induced damage in rock salt, which should be addressed. Thermal stressing of rock samples has been carried out by many authors on a variety of other rock types (e.g. Fredrich & Wong 1986; Browning *et al.* 2017; Castagna *et al.* 2018; Daoud *et al.* 2020), but these are usually analysing processes related to magmatic systems and therefore the temperatures, and temperature gradients (up to several hundred degrees Celsius), are much higher than those likely to exist in UGS operations. The other difference is that many of these experiments only investigate the effects on

mechanical properties and/or damage (indirectly) over one, or minimal heating and cooling cycles.

Therefore, further work investigating the potential of damage over more modest temperature fluctuations (tens of degrees Celsius), longer time frames (weeks to months) containing multiple heating and cooling cycles (hundreds to thousands) should be carried out on samples of rock salt. These testing conditions would better replicate the operational conditions relevant for UGS and improve our understanding of the risks that thermally induced damage may cause. Experimental work should include the monitoring of damage (through acoustic emissions and/or ultrasonic wave velocities), and permeability measurements.

5.4 Temporary storage of CO_2

Although salt caverns have been used to store numerous fluids, the idea to temporarily store CO_2 is relatively recent, and has only really been considered as a temporary solution until more suitable permanent storage reservoirs are discovered or prepared (Dusseault *et al.* 2004; Likar *et al.* 2015). However, high purity CO_2 is an essential product in some industries (Chauvy & De Weireld 2020). For such cases, temporary storage of CO_2 derived from heavy industries (where CO_2 emissions are unavoidable) in salt caverns presents a unique opportunity to turn what has historically been a harmful by-product into a useful commodity. Ideally, CO_2 emitters, temporary storage facilities, and end users should be located close together to avoid unnecessary transport of CO_2, and areas where this occurs are termed net-zero carbon clusters. ConsenCUS, which is a European funded H2020 project (https://consencus.eu/), aims to demonstrate the feasibility of such a supply chain and net-zero carbon clusters, for three case studies in Europe.

For net-zero carbon clusters, both the supply and demand of CO_2 will dictate the operational parameters (injection/production cycle frequency, injection/production flow rates), whereas the local geology will dictate the storage volumes available. It is likely, that the operational parameters of the temporary storage of CO_2 in salt caverns will be more akin to those of CAES or hydrogen storage (i.e., daily or hourly discharge and recharge), rather than the seasonal storage of natural gas.

Given that this supply chain is a relatively new concept, there is much work to be done on understanding how to match the supply and demand of CO_2 with available temporary storage in the subsurface. This is one of the main goals of the ConsenCUS project.

6 References

Berest, P., Brouard, B. & Durup, G. 1996. Behavior of Sealed Solution-mined Caverns.

Berest, P., Bergues, J., Brouard, B., Durup, J.G. & Guerber, B. 2001. *A Salt Cavern Abandonment Test*.

Berest, P., Brouard, B. & Karimi-Jafari, M. 2005. Deep salt caverns abandonment. *In*: *Post-Mining*. Nancy, France.

Bérest, P. 2011. Thermomechanical aspects of high frequency cycling in salt storage caverns. *International Gas Research Conference Proceedings*, **2**, 1603–1624.

Bérest, P. 2019. Heat transfer in salt caverns. *International Journal of Rock Mechanics and Mining Sciences*, **120**, 82–95, https://doi.org/10.1016/j.ijrmms.2019.06.009.

Bérest, P. & Brouard, B. 2014. Long-Term Behavior of Salt Caverns. U.S. Rock Mechanics/Geomechanics Symposium.

Birch, F. 1960. The velocity of compressional waves in rocks to 10 kilobars, Part 1. *Journal of Geophysical Research*, **65**, 1083–1102.

Böttcher, N., Görke, U.J., Kolditz, O. & Nagel, T. 2017. Thermo-mechanical investigation of salt caverns for short-term hydrogen storage. *Environmental Earth Sciences*, **76**, https://doi.org/10.1007/s12665-017-6414-2.

Brouard, B., Bérest, P., De Greef, V., Béraud, J.F., Lheur, C. & Hertz, E. 2013. Creep closure rate of a shallow salt cavern at Gellenoncourt, France. *International Journal of Rock Mechanics and Mining Sciences*, **62**, 42–50, https://doi.org/10.1016/j.ijrmms.2012.12.030.

Browning, J., Meredith, P.G., Stuart, C.E., Healy, D., Harland, S. & Mitchell, T.M. 2017. Acoustic characterization of crack damage evolution in sandstone deformed under conventional and true triaxial loading. *Journal of Geophysical Research: Solid Earth*, **122**, 4395–4412, https://doi.org/10.1002/2016JB013646.

Caglayan, D.G., Weber, N., Heinrichs, H.U., Linßen, J., Robinius, M., Kukla, P.A. & Stolten, D. 2020. Technical potential of salt caverns for hydrogen storage in Europe. *International Journal of Hydrogen Energy*, **45**, 6793–6805, https://doi.org/10.1016/j.ijhydene.2019.12.161.

Carter, N.L. & Hansen, F.D. 1983. Creep of rocksalt. *Tectonophysics*, **92**, 275–333, https://doi.org/10.1016/0040-1951(83)90200-7.

Carter, N.L., Horseman, S.T., Russell, J.E. & Handin, J. 1993. *Rheology of Rocksalt*.

Castagna, A., Ougier-Simonin, A., Benson, P.M., Browning, J., Walker, R.J., Fazio, M. &

Vinciguerra, S. 2018. Thermal Damage and Pore Pressure Effects of the Brittle-Ductile Transition in Comiso Limestone. *Journal of Geophysical Research: Solid Earth*, **123**, 7644–7660, https://doi.org/10.1029/2017JB015105.

Chauvy, R. & De Weireld, G. 2020. CO2 Utilization Technologies in Europe: A Short Review. *Energy Technology*, **8**, https://doi.org/10.1002/ente.202000627.

Chen, J., Peng, H., Fan, J., Zhang, X., Liu, W. & Jiang, D. 2020. Microscopic investigations on the healing and softening of damaged salt by uniaxial deformation from CT, SEM and NMR: Effect of fluids (brine and oil). *RSC Advances*, **10**, 2877–2886, https://doi.org/10.1039/c9ra05866d.

Commission, E. 2021. 2030 climate & energy frameworkhttps://ec.europa.eu/clima/eu-action/climate-strategies-targets/2030-climate-energy-framework_en.

Cornet, J.S., Dabrowski, M. & Schmid, D.W. 2018. Long term creep closure of salt cavities. *International Journal of Rock Mechanics and Mining Sciences*, **103**, 96–106, https://doi.org/10.1016/j.ijrmms.2018.01.025.

Cosenza, P. & Ghoreychi, M. 1999. Effects of very low permeability on the long-term evolution of a storage cavern in rock salt. *International Journal of Rock Mechanics and Mining Sciences*, **36**, 527–533, https://doi.org/10.1016/S0148-9062(99)00018-2.

Cosenza, P., Ghoreychi, M., Bazargan-Sabet, B. & Marsily, G. de. 1999. In situ rock salt permeability measurement for long term safety assessment of storage. *International Journal of Rock Mechanics and Mining Sciences and Geomechanics Abstracts*, **4**, 509–526.

Covey-Crump, S.J., Xiao, W.F., Mecklenburgh, J., Rutter, E.H. & May, S.E. 2016. Exploring the influence of loading geometry on the plastic flow properties of geological materials: Results from combined torsion + axial compression tests on calcite rocks. *Journal of Structural Geology*, **88**, 20–31, https://doi.org/10.1016/J.JSG.2016.04.007.

Cristescu, N. & Hunsche, U. 1998. Time effects in rock mechanics. 342.

Crotogino, F., Mohmeyer, K.-U. & Scharf, R. 2001. Huntorf CAES: More than 20 Years of Successful Operation.

Daoud, A., Browning, J., Meredith, P.G. & Mitchell, T.M. 2020. Microstructural Controls on Thermal Crack Damage and the Presence of a Temperature-Memory Effect During Cyclic Thermal Stressing of Rocks. *Geophysical Research Letters*, **47**, 1–11, https://doi.org/10.1029/2020GL088693.

Djahanguiri, F. & Matthews, S.C. 1983. Geotechnical considerations for design of nuclear repository in bedded salt in the US. *In*: *Six International Symposium on Salt*.

Djizanne, H. 2014. *Stabilité Mécanique d'une Cavité Saline Soumise à Des Variations Rapides de Pression: Application Au Stockage Souterrain de Gaz Naturel, d'air Comprimé et*

d'hydrogène . Ecole Doctorale Polytechnique.

Donadei, S. & Schneider, G.S. 2016. Compressed Air Energy Storage in Underground Formations. *Storing Energy: With Special Reference to Renewable Energy Sources*, 113–133, https://doi.org/10.1016/B978-0-12-803440-8.00006-3.

Dusseault, M.B., Bachu, S. & Rothenburg, L. 2004. Sequestration of CO2 in salt caverns. *Journal of Canadian Petroleum Technology*, **43**, 49–55, https://doi.org/10.2118/04-11-04.

Evans, D., Parkes, D., et al. 2021. Salt Cavern Exergy Storage Capacity Potential of UK Massively Bedded Halites, Using Compressed Air Energy Storage (CAES). *Applied Sciences 2021, Vol. 11, Page 4728*, **11**, 4728, https://doi.org/10.3390/APP11114728.

Evans, D.J., Williams, J.D.O., Hough, E. & Stacey, A. 2011. The stratigraphy and lateral correlations of the Northwich and Preesall halites from the Cheshire Basin-East Irish Sea areas: implications for sedimentary environments , rates of deposition and the solution mining of gas storage caverns. *SMRI Fall 2011 Technical Conference*, 1–28.

Fan, J., Chen, J., Jiang, D., Ren, S. & Wu, J. 2016. Fatigue properties of rock salt subjected to interval cyclic pressure. *International Journal of Fatigue*, **90**, 109–115, https://doi.org/10.1016/j.ijfatigue.2016.04.021.

Forsberg, C.W. 2006. Assessment of nuclear-hydrogen synergies with renewable energy systems and coal liquefaction processes. ORNL/TM-2006/114, August.

Frankel, J., Rich, F.J. & Homan, C.G. 1976. Acoustic Velocities in Polycrystalline NaCl at 300 K Measured at Static Pressures from 25 to 27 kbar. *Journal of Geophysical Research*.

Fredrich, J.T. & Wong, T. 1986. Micromechanics of thermally induced cracking in three crustal rocks. *Journal of Geophysical Research: Solid Earth*, **91**, 12743–12764, https://doi.org/10.1029/jb091ib12p12743.

Fuenkajorn, K. & Phueakphum, D. 2010. Effects of cyclic loading on mechanical properties of Maha Sarakham salt. *Engineering Geology*, **112**, 43–52, https://doi.org/10.1016/j.enggeo.2010.01.002.

Fuenkajorn, K. & Phueakphum, D. 2011. Laboratory assessment of healing of fractures in rock salt. *Bulletin of Engineering Geology and the Environment*, **70**, 665–672, https://doi.org/10.1007/s10064-011-0370-y.

Gevantman, L.H., Lorenz, J., Haas, J.L., Clynne, M.A., Potter, R.W. & Schafer, C.M. 1981. *Physical Properties Data for Rock Salt*, https://doi.org/10.6028/NBS.MONO.167.

Giambastiani, M. 2020. Geomechanical Characterization of Evaporitic Rocks. *Soft Rock Mechanics and Engineering*, 129–161, https://doi.org/10.1007/978-3-030-29477-9_6.

Gloyna, E.F. & Reynolds, T.D. 1961. Permeability measurements of rock salt. *Journal of Geophysical Research*, **66**, 3913–3921, https://doi.org/10.1029/JZ066I011P03913.

Gretz, J., Drolet, B., Kluyskens, D., Sandmann, F. & Ullmann, O. 1994. Status of the hydro-

hydrogen pilot project (EQHHPP). *International Journal of Hydrogen Energy*, **19**, 169–174, https://doi.org/10.1016/0360-3199(94)90123-6.

Gudmundsson, A. 2011. *Rock Fractures in Geological Processes*. Cambridge, Cambridge University Press.

Günther, R.M., Salzer, K., Popp, T. & Lüdeling, C. 2015. Steady-State Creep of Rock Salt: Improved Approaches for Lab Determination and Modelling. *Rock Mechanics and Rock Engineering*, **48**, 2603–2613, https://doi.org/10.1007/S00603-015-0839-2/FIGURES/7.

Hatzor, Y.H. & Heyman, E.P. 1997. Dilation of anisotropic rock salt: Evidence from Mount Sedom diapir. *Journal of Geophysical Research: Solid Earth*, **102**, 14853–14868, https://doi.org/10.1029/97JB00958.

He, W., Luo, X., Evans, D., Busby, J., Garvey, S., Parkes, D. & Wang, J. 2017. Exergy storage of compressed air in cavern and cavern volume estimation of the large-scale compressed air energy storage system. *Applied Energy*, **208**, 745–757, https://doi.org/10.1016/j.apenergy.2017.09.074.

Huang, X. & Xiong, J. 2011. Numerical simulation of gas leakage in bedded salt rock storage cavern. *Procedia Engineering*, **12**, 254–259, https://doi.org/10.1016/j.proeng.2011.05.040.

Hudec, M.R. & Jackson, M.P.A. 2007. Terra infirma: Understanding salt tectonics. *Earth-Science Reviews*, **82**, 1–28, https://doi.org/10.1016/J.EARSCIREV.2007.01.001.

Hunsche, U. & Hampel, A. 1999. Rock salt - The mechanical properties of the host rock material for a radioactive waste repository. *Engineering Geology*, **59**, 271–291, https://doi.org/10.1016/s0013-7952(99)00011-3.

IPCC. 2014. *Climate Change 2014 Mitigation of Climate Change*, https://doi.org/10.1017/cbo9781107415416.

Jeremic, M.L. (Michael L.. 1994. Rock mechanics in salt mining. 532.

Judd, R. & Pinchbeck, D. 2016. Hydrogen admixture to the natural gas grid. *Compendium of Hydrogen Energy*, 165–192, https://doi.org/10.1016/B978-1-78242-364-5.00008-7.

Khaledi, K., Mahmoudi, E., Datcheva, M. & Schanz, T. 2016. Stability and serviceability of underground energy storage caverns in rock salt subjected to mechanical cyclic loading. *International Journal of Rock Mechanics and Mining Sciences*, **86**, 115–131, https://doi.org/10.1016/j.ijrmms.2016.04.010.

King, M., Jain, A., Bhakar, R., Mathur, J. & Wang, J. 2021. Overview of current compressed air energy storage projects and analysis of the potential underground storage capacity in India and the UK. *Renewable and Sustainable Energy Reviews*, **139**, 110705, https://doi.org/10.1016/j.rser.2021.110705.

Kruck, O., Crotogino, F., Prelicz, R. & Rudolph, T. 2013. *Overview on All Known Underground Storage Technologies for Hydrogen*.

Landinger, H. & Crotogino, F. 2007. The role of large-scale hydrogen storage for future renewable energy utilisation. *In*: *Second International Renewable Energy Storage Conference (IRES II)*.

Landinger, H., Bunger, U., Raksha, T., Weindorf, W., Simon, J., Correas, L. & Crotogino, F. 2013. *Update of Benchmarking of Large Scale Hydrogen Underground Storage with Competing Options:*

Leet, L.D. & Birch, F. 1942. Seismic Velocities. *Special Paper of the Geological Society of America*, **36**, 93–101, https://doi.org/10.1130/SPE36-P93.

Leith, W. 2000. Geologic and engineering constraints on the feasibility of clandestine nuclear testing by decoupling in large underground cavities. *Open-File Report*, https://doi.org/10.3133/OFR0128.

Leuger, B., Staudtmeister, K. & Zapf, D. 2012. The thermo–mechanical behavior of a gas storage cavern during high frequency loading. *In*: *Mechanical Behavior of Salt VII*.

Li, H., Dong, Z., Yang, Y., Liu, B., Chen, M. & Jing, W. 2018. Experimental Study of Damage Development in Salt Rock under Uniaxial Stress Using Ultrasonic Velocity and Acoustic Emissions. *Applied Sciences 2018, Vol. 8, Page 553*, **8**, 553, https://doi.org/10.3390/APP8040553.

Liang, W., Yang, C., Zhao, Y., Dusseault, M.B. & Liu, J. 2007. Experimental investigation of mechanical properties of bedded salt rock. *International Journal of Rock Mechanics and Mining Sciences*, **44**, 400–411, https://doi.org/10.1016/J.IJRMMS.2006.09.007.

Liang, W., Zhang, C., Gao, H., Yang, X., Xu, S. & Zhao, Y. 2012. Experiments on mechanical properties of salt rocks under cyclic loading. *Journal of Rock Mechanics and Geotechnical Engineering*, **4**, 54–61, https://doi.org/10.3724/SP.J.1235.2012.00054.

Likar, J., Zarn, J., Grov, E., Cebasek, T.M. & Likar, A. 2015. CO2 temporary storage in big underground caverns. *RMZ - Materials & Geoenvironment*.

Ma, L.J., Liu, X.Y., et al. 2013. Experimental investigation of the mechanical properties of rock salt under triaxial cyclic loading. *International Journal of Rock Mechanics and Mining Sciences*, **62**, 34–41, https://doi.org/10.1016/j.ijrmms.2013.04.003.

Martin-Clave, C. 2021. *Impact of Second Phase Content over Rheological Behaviour of Rock Salt under Cyclic Loading Conditions Applied to Underground Gas Storage*. University of Nottingham., https://doi.org/10.1007/s00603-021-02449-4.

Martin-Clave, C., Ougier-Simonin, A. & Vandeginste, V. 2021. Impact of Second Phase Content on Rock Salt Rheological Behavior Under Cyclic Mechanical Conditions. *Rock Mechanics and Rock Engineering*, https://doi.org/10.1007/s00603-021-02449-4.

Mavko, G., Mukerji, T. & Dvorkin, J. 2009. *The Rock Physics Handbook*, Second. Cambridge University Press.

Mellegard, K. & Dusterloh, U. 2012. *High Frequency Cycling of Gas Storage Caverns: Phase Ii: Cyclical Loading Effects on the Damage and Creep Properties of Salt*.

Melvin, J.L. 1991. Evaporites, petroleum, and mineral resources. 556.

Michalski, J., Bünger, U., et al. 2017. Hydrogen generation by electrolysis and storage in salt caverns: Potentials, economics and systems aspects with regard to the German energy transition. *International Journal of Hydrogen Energy*, **42**, 13427–13443, https://doi.org/10.1016/J.IJHYDENE.2017.02.102.

Minkley, W. & Muhlbauer, J. 2007. Constitutive models to describe the mechanical behavior of salt rocks and the imbedded weakness planes Comparison of current constitutive models and simulation procedures on the basis of model calculations of the thermo-mechanical behavior and healing of. *In*: *6th Conference on the Mechanical Behavior of Salt*.

Mokhatab, S., Poe, W.A. & Mak, J.Y. 2018. *Handbook of Natural Gas Transmission and Processing: Principles and Practices*. Elsevier Science.

Morgan, M.T. 1979. *Thermal Conductivity of Rock Salt from Louisiana Salt Domes*.

Munson, D.E. 1979. Preliminary deformation-mechanism map for salt (with application to WIPP), https://doi.org/10.2172/6499296.

Ngo, D.T. & Pellet, F.L. 2018. Numerical modeling of thermally-induced fractures in a large rock salt mass. *Journal of Rock Mechanics and Geotechnical Engineering*, **10**, 844–855, https://doi.org/10.1016/j.jrmge.2018.04.008.

Nieland, J.D. 2008. Salt cavern Thermodynamics-Comparison Between Hydrogen, Natural Gas and Air Storage. *In*: *SMRI Fall Meeting*. Austin, Texas.

Ochsenius, C. 1877. *Die Bildung Der Steinsalzlager Und Ihrer Mutterlaugensalze : Unter Spezieller Berücksichtigung Der Flötze von Douglashall in Der Egeln'schen Mulde.* Halle, Halle, 1877.

Özkan, I., Özarslan, A., Genis, M. & Özşen, H. 2009. Assessment of Scale Effects on Uniaxial Compressive Strength in Rock Salt. *Environmental and Engineering Geoscience*, **15**, 91–100, https://doi.org/10.2113/GSEEGEOSCI.15.2.91.

Panfilov, M. 2016. Underground and pipeline hydrogen storage. *Compendium of Hydrogen Energy*, 91–115, https://doi.org/10.1016/B978-1-78242-362-1.00004-3.

Parkes, D., Evans, D.J., Williamson, P. & Williams, J.D.O. 2018. Estimating available salt volume for potential CAES development: A case study using the Northwich Halite of the Cheshire Basin. *Journal of Energy Storage*, **18**, 50–61, https://doi.org/10.1016/j.est.2018.04.019.

Peach, C. 1991. *Influence of Deformation on the Fluid Transport Properties of Salt Rocks*.

Peach, C.J., Spiers, C.J. & Trimby, P.W. 2001. Effect of confining pressure on dilatation, recrystallization, and flow of rock salt at 150°C. *Journal of Geophysical Research: Solid*

Earth, **106**, 13315–13328, https://doi.org/10.1029/2000JB900300.

Popp, T., Kern, H. & Schulze, O. 2001. Evolution of dilatancy and permeability in rock salt during hydrostatic compaction and triaxial deformation. *Journal of Geophysical Research: Solid Earth*, **106**, 4061–4078, https://doi.org/10.1029/2000JB900381.

Prasse, P., Wookey, J., Kendall, J.M., Roberts, D. & Dutko, M. 2020. Seismic anisotropy in deforming halite: evidence from the Mahogany salt body. *Geophysical Journal International*, **223**, 1672–1687, https://doi.org/10.1093/GJI/GGAA402.

Raymer, D.G., Tommasi, A. & Kendall, J.M. 2000. Predicting the seismic implications of salt anisotropy using numerical simulations of halite deformationSeismic Implications of Salt Anisotropy. *Geophysics*, **65**, 1272–1280, https://doi.org/10.1190/1.1444818.

Schenk, O.O. & Urai, J.L. 2004. Microstructural evolution and grain boundary structure during static recrystallization in synthetic polycrystals of sodium chloride containing saturated brine. *Contributions to Mineralogy and Petrology*, **146**, 671–682, https://doi.org/10.1007/S00410-003-0522-6/FIGURES/12.

Schulze, O., Popp, T. & Kern, H. 2001. Development of damage and permeability in deforming rock salt. *Engineering Geology*, **61**, 163–180, https://doi.org/10.1016/S0013-7952(01)00051-5.

Senseny, P.E., Hansen, F.D., Russell, J.E., Carter, N.L. & Handin, J.W. 1992. Mechanical behaviour of rock salt: Phenomenology and micromechanisms. *International Journal of Rock Mechanics and Mining Sciences & Geomechanics Abstracts*, **29**, 363–378, https://doi.org/10.1016/0148-9062(92)90513-Y.

Shen, X., Arson, C., Ding, J., Chester, F.M. & Chester, J.S. 2020. Mechanisms of Anisotropy in Salt Rock Upon Microcrack Propagation. *Rock Mechanics and Rock Engineering*, **53**, 3185–3205, https://doi.org/10.1007/S00603-020-02096-1.

Sicsic, P. & Bérest, P. 2014. Thermal cracking following a blowout in a gas-storage cavern. *International Journal of Rock Mechanics and Mining Sciences*, **71**, 320–329, https://doi.org/10.1016/j.ijrmms.2014.07.014.

Singh, A., Kumar, C., Kannan, L.G., Rao, K.S. & Ayothiraman, R. 2017. Rheological Behaviour of Rock Salt Under Uniaxial Compression. *Procedia Engineering*, **173**, 639–646, https://doi.org/10.1016/J.PROENG.2016.12.122.

Singh, T.N., Kainthola, A. & Venkatesh, A. 2012. Correlation between point load index and uniaxial compressive strength for different rock types. *Rock Mechanics and Rock Engineering*, **45**, 259–264, https://doi.org/10.1007/S00603-011-0192-Z/TABLES/4.

Spiers, C.J., Schutjens, P.M.T.M., Brzesowsky, R.H., Peach, C.J., Liezenberg, J.L. & Zwart, H.J. 1990. Experimental determination of constitutive parameters governing creep of rocksalt by pressure solution. *Geological Society Special Publications*.

Staudtmeister, K., Zapf, D., Leuger, B. & Elend, M. 2017. Temperature Induced Fracturing of Rock Salt Mass. *In*: *Procedia Engineering*. Elsevier Ltd, 967–974., https://doi.org/10.1016/j.proeng.2017.05.268.

Steeb, H. & Abaoud, H. 1996. *HYSOLAR German Saudi Joint Program on Solar Hydrogen Production and Utilization ; Phase II 1992 - 1995*.

Stormont, J.C. 1997. In situ gas permeability measurements to delineate damage in rock salt. *International Journal of Rock Mechanics and Mining Sciences*, **34**, 1055–1064, https://doi.org/10.1016/S1365-1609(97)90199-4.

Stormont, J.C. & Daemen, J.J.K. 1992. Laboratory study of gas permeability changes in rock salt during deformation. *International Journal of Rock Mechanics and Mining Sciences & Geomechanics Abstracts*, **29**, 325–342, https://doi.org/10.1016/0148-9062(92)90510-7.

Szyszka, A. 1990. Realization of the Solar-Hydrogen project at Neunburg Vorm Wald, F. R. G. *International Journal of Hydrogen Energy*, **15**, 597–599.

Tarkowski, R. 2019. Underground hydrogen storage: Characteristics and prospects. *Renewable and Sustainable Energy Reviews*, **105**, 86–94, https://doi.org/10.1016/J.RSER.2019.01.051.

Tixier, M.P. & Alger, R.P. 1970. Log evaluation of nonmetallic mineral deposits. *Geophysics*, **35**, 124–142, https://doi.org/10.1190/1.1440070.

Urai, J.L., Schléder, · Z, Spiers, · C J & Kukla, P.A. 2008. Chapter 5.2 Flow and Transport Properties of Salt Rocks. *In*: *Dynamics of Complex Intracontinental Basins: The Central European Basin System*. 277–290.

Van Sambeek, L.L., Ratigan, J.L. & Hansen, F.D. 1993. Dilatancy of rock salt in laboratory tests. *International Journal of Rock Mechanics and Mining Sciences & Geomechanics Abstracts*, **30**, 735–738, https://doi.org/10.1016/0148-9062(93)90015-6.

Vernik, L. & Liu, X. 1997. Velocity anisotropy in shales: A petrophysical study. *Geophysics*, **62**, 521–532, https://doi.org/10.1190/1.1444162.

Voronov, F.F. & Grigor'ev, S.B. 1971. Velocity of sound in cesium chloride and sodium chloride at pressures up to 100 kbars. *Soviet Physics Doklady*. Vol. 15., p. 1126

Walsh, J.B. 1981. Effect of pore pressure and confining pressure on fracture permeability. *International Journal of Rock Mechanics and Mining Sciences and*, **18**, 429–435, https://doi.org/10.1016/0148-9062(81)90006-1.

Wang, T., Yan, X., Yang, H., Yang, X., Jiang, T. & Zhao, S. 2013. A new shape design method of salt cavern used as underground gas storage. *Applied Energy*, **104**, 50–61, https://doi.org/10.1016/J.APENERGY.2012.11.037.

Warren, J.K. 2016. *Evaporites*. Cham, Springer International Publishing, https://doi.org/10.1007/978-3-319-13512-0.

Xing, W., Zhao, J., Hou, Z., Were, P., Li, M. & Wang, G. 2015. Horizontal natural gas caverns in thin-bedded rock salt formations. *Environmental Earth Sciences*, **73**, 6973–6985, https://doi.org/10.1007/S12665-015-4410-Y/FIGURES/15.

Yang, L., Huang, J. nan & Zhou, F. 2020. Thermophysical properties and applications of nano-enhanced PCMs: An update review. *Energy Conversion and Management*, **214**, 112876, https://doi.org/10.1016/J.ENCONMAN.2020.112876.

Yin, H. 1992. Acoustic velocity and attenuation of rocks : isotropy, intrinsic anisotropy, and stress-induced anisotropy. *undefined*.

Yin, H., Yang, C., et al. 2019. Study on Damage and Repair Mechanical Characteristics of Rock Salt Under Uniaxial Compression. *Rock Mechanics and Rock Engineering*, **52**, 659–671, https://doi.org/10.1007/S00603-018-1604-0/FIGURES/14.

Zong, J., Stewart, R.R., Dyaur, N. & Myers, M.T. 2017. Elastic properties of rock salt: Laboratory measurements and Gulf of Mexico well-log analysis, https://doi.org/10.1190/GEO2016-0527.1.